Table of contents

1. Introduction

Almost as soon as digital computers became available, it was realized that they could be used to process and extract information from digitized images. Initially, work on digital image analysis dealt with specific classes of images such as text, photomicrographs, nuclear particle tracks, and aerial photographs; but by the 1960s, general algorithms and paradigms for image analysis began to be formulated. When the artificial intelligence community began to work on robot vision, these paradigms were extended to include recovery of three−dimensional information, at first from single images of a scene, but eventually from image sequences obtained by a moving camera; at this stage, image analysis had become scene analysis or computer vision. An ’existence proof’ for the feasibility of computer vision tasks is that animals and humans use vision quite effectively in the real world. A possible basis for this is that biological visual systems make use of redundant visual data and process it on redundant ’pathways’. Computer vision systems usually avoid such redundancy in order to reduce computational cost. History of digital image processing over the past half−century led to many elegant mathematical models and algorithms, as well. Real−world visual domains do not satisfy simple mathematical or probabilistic models. The inadequacy of scene models does not imply that computer vision systems will never perform adequately. Indeed, in many areas of application, successful image analysis and computer vision systems have been developed and marketed, even though the classes of scenes involved can be modeled only crudely, and the systems generally make use of *ad hoc* methods (A. Rosenfeld, 2000).

There is a growing interest in the grain industry for on−line monitoring of grain. Rapid evaluation of the content of a sample can be used to develop optimum cleaning strategies, make appropriate decisions, and for complete automation of certain operations. Such monitoring would result in increased throughput and enhanced recovery of salvageable grains. A sample of grain may contain seeds of several species and numerous type of impurities. The machine vision system should identify the primary grain from other materials present in a sample. The positive identification of the primary grain and determination of the fractions of small and large seeds in a sample is important in automating the controls of grain cleaning machinery (Shatadal *et.al.*, 1995). In addition, grain−throughput of the combine and the loss of grain at this throughput are used to determine performance of grain harvesting machines. Portion of broken kernels in the separated grain is another important quality criteria in this case (Schneider, Häußer, Kutzbach, 1997). The mentioned quality parameters are usually measured by visual inspection. This type of evaluation takes too long, and allocates valuable human resources (requires well−trained people with experience). Computerized image analysis is an objective and nondestructive method for measurement of morphometrical features such as shape, size, color and surface texture. It allows experts to describe visible attributes accurately. The importance of such support appears in the national and international standards and directives, where hand−picking is still the most important argument in the evaluation of purity of incoming or outgoing cereals.

2. Literature

2.1. Standards

2.1.1. Hungarian standards for grain inspection

Methodology for inspection of foreign materials is defined in the MSZ 6354/1−2 and MSZ 6367−2 standards in Hungary. This analysis is based on hand−picking. Equipment can help in advance assorting (bolter, aspirator, mixer). The following table presents minimum required sample size and maximum quantity of grain to be represented by a sample:

Table 1: Sample size requirements of the standard MSZ 6354/2−82

Maximum quantity of one unit		Base	Laboratory		Evaluation	
		Minimum sample size				
Hungarian kg	International kg	kg	Hungarian g	International g	Hungarian g	International g
25000	25000	10	1000	1000	100	120

The quality report contains weight of the sample, name of the varieties and the number of kernels examined. Two parallel measurements have to be performed. The standard defines the maximum acceptable deviation from the average value. Limits were computed according to the expected differences without any error in the measurement.

Table 2: Quality requirements of wheat standard MSZ 6383

Quality requirements	Common wheat				Durum wheat	
	extra quality	in milling industry				
		I.	II.	III.	I.	II.
Test weight, kg/100 l	78	76		72	78	75
Moisture content, %	14.5	14.5		14.5	14.5	14.5
Mixed materials, %	2.0	2.0		2.0	2.0	2.0
− adverse materials %	0.5	0.5		0.5	0.5	0.5
− light mixture %	0.5	0.5		0.5	0.5	0.5
Over the 2.0 % allowed:						
− broken grain, %	2.0	2.0		6.0	2.0	2.0
− germinated, %	2.0	2.0		5.0	2.0	2.0
− rye, %	2.0	2.0		3.0	−	−
− defective kernels, %	2.0	2.0		2.0	3.0	3.0
− discolored kernels, %	−	−		−	3.0	8.0
− chinch attacked, % *	−	2		4	2	2
− common wheat, %	−	−		−	4.0	10
Vitreous at least, % *	−	−			60	30
Fragments of insects	NOT ALLOWED					
* Number of kernels of certain attribute						

Adverse materials are inorganic or organic materials with negative effect on food product or toxic seeds (weeds, blighted or mold damaged kernels: *Datura stramonium, Conium maculatum, Claviceps purpurea, etc.*). Defective kernels cannot be used in food production and are restricted in forage as well. Vitreosity tests are important in Hungary and have had significance since 1968. This quality parameter depends on the composition, structure and hardness of the endosperm.

Abnormal odor in cereals means:

- smell of alcoholic fermentation or fermentation of lactic, acetic or butyric acid
- musty or close air (probably as a result of mold damage)
- sour smell because of the oxidative changes of fat
- smell of chemicals, inorganic oil, other plants

2.1.2. Grain inspection in the United States

The Grain Inspection, Packers and Stockyards Administration, Federal Grain Inspection Service (FGIS), an agency of the United States Department of Agriculture (USDA), helps to move grain into the market place by providing farmers, grain handlers, processors, exporters, and international buyers with information that accurately and consistently describes the quality and quantity of grain being bought and sold. The official inspection and weighing system is a unique public−private partnership overseen by FGIS. The system includes Federal offices and States and private agencies authorized by FGIS to provide official inspection and weighing service to the domestic and export grain trade. The Official United States Standards for Grain provide the criteria for determining the kind, class, and condition of grain. The standards also define quality and condition factors and set grade limits based on factor determinations. Quality factors, which vary by grain, include test weight, damaged kernels, and foreign materials. Condition factors include heating, objectionable odor, and insect infestation. It is important to note that the Official United States Standards for Grain are not seasonally adjusted, regardless of average new crop quality.

The process of inspecting grain begins with sampling and usually follows a prescribed path whether the grain is being inspected for grade or for factors only. First, the sample is examined for objectionable odor, insect infestation, and other harmful or unusual conditions. Then, a portion of grain is divided out from the sample and its moisture content is determined. The sample may next be tested for dockage, followed by a test weight determination. For some grains, test weight is determined before dockage. After this, the sample is divided into small portions; and the portions are examined for other factors, such as damaged kernels and foreign material. All equipment are tested at least twice a year against known standards and are adjusted as needed. When reducing samples in size or dividing factor portions from samples, Boerner dividers or any other devices that gives equivalent results are used. The recommended minimum portion sizes are as follows:

Table 3: Recommended minimum portion sizes by FGIS

	Barley	Corn	Oats	Sorghum	Soybeans	Wheat
	Portion weights in grams					
Damage	15	125	30	15	125	15
Dockage	250	N/A	N/A	250	N/A	250
Foreign material	30	250	30	250	125	30
Heating	The lot as a whole					
Infestation	The original sample or lot as a whole					
Moisture	Amount recommended by the instrument manufacturer					
Objectionable odors	The original sample or lot as a whole					
Oil	Amount recommended by the instrument manufacturer					
Protein	Amount recommended by the instrument manufacturer					
Test weight	Amount recommended by the instrument manufacturer					

For other types of grain, the portion sizes recommended for a grain of similar size are used. Grain that is contaminated by harmful substances is graded as "U.S. Sample grade." To be

considered "contaminated," the original sample must contain:

- Animal filth (e.g., excreta)
    - corn: animal filth in excess of 0.20 %.
    - barley, flaxseed, oats, sorghum, soybeans, and sunflower seed: 10 or more rodent pellets, bird droppings, or an equal quantity of other animal filth.
    - rye, triticale, and wheat: 2 or more rodent pellets, bird droppings, or an equal quantity of other animal filth.
- Castor Beans
    - All grains except canola: 2 or more castor beans.
- Cockleburs
    - barley, corn, flaxseed, and sorghum: 8 or more cockleburs or similar seeds.
- Crotalaira Seeds
    - All grains, except canola: 3 or more crotalaria seeds
- Distinctly low quality
    - All grains: when a lot of grain is of inferior quality because of an unusual state or condition and it cannot be graded properly using the grading factors provided in the standards.
- Glass
    - All Grains, except wheat and canola: 2 or more pieces of glass.
    - wheat and canola: 1 or more pieces of glass.
- Stones
    - barley, rye, and triticale: 8 or more stones or any number of stones which have an aggregate weight in excess of 0.2 % of the sample weight.
    - flaxseed, oats, sorghum, soybean and sunflower seed: 8 or more stones which have an aggregate weight in excess of 0.2 % of the sample weight.
    - corn: 1 or more stones which have an aggregate weight in excess of 0.1 % of the sample weight.
    - wheat: 4 or more stones or any number of stones which have an aggregate weight in excess of 0.1 % of the sample weight.
- Unknown foreign substance
    - All grains, except canola: 4 or more particles of an unknown foreign substance, including rock salt or crystalline substances, or a commonly recognized harmful or toxic substance, including so−called "pink wheat."
    - canola: 2 or more particles of an unknown foreign substance, including rock salt or crystalline substances, or a commonly recognized harmful or toxic substance.

Wheat that contains a total of 5 or more particles of any harmful substances should be considered "contaminated" and graded "U.S. Sample grade." The amount of foreign material in canola, flaxseed, mixed grain, mustard seed, rapeseed, or sunflower seed is not usually determined. Foreign materials are:

- for barley: all matter other than barley, other grains, and wild oats that remains in the sample after the removal of dockage.
- for corn: all matter that passes readily through a 12/64−inch round−hole sieve and all matter other than corn that remains in the sample after sieving.
- for rye and triticale: all matter other than rye (or triticale) that remains in the sample after the removal of dockage.
- for soybeans: all matter that passes through an 8/64−inch round−hole sieve, and all matter other than soybeans that remains in the sample after sieving.
- for wheat: all matter other than wheat that remains in the sample after the removal of dockage and shrunken and broken kernels.

Determination of foreign materials is done by mechanical dockage tester (corn, sorghum, sunflower seed), hand sieves (corn, oats, sorghum, soybeans) or handpicking (barley, oats, rye, triticale, sorghum, soybeans, sunflower seed, wheat).

The most common types of kernel damage are germ−, frost−, immature−, heat−, mold−, scab−, sprout−, insect−, ground−, and cob rot−damage. Most of these types of damage result in some sort of discoloration or change in kernel texture. If two or more insect−damaged kernels are found in a 15 g portion of wheat, a second 15 g portion is examined. If two or more insect−damaged kernels are found in the second portion, a 70 g portion is examined and then the number of insect−damaged kernels found in all three portions are combined. If 32 or more insect−damaged kernels are found in the combined portions (i.e., 100 grams) the wheat is classed "U.S. Sample grade." If fewer than two insect−damaged kernels are found in either the first or second portion, the examination is discontinued.

Table 4: Characteristics of damages according to US Grain Standard Acts

Type of damage	Characteristics
Black Tip Fungus−Damaged Kernels (wheat)	Kernels with black tip fungus growth on the germ and in the crease of the kernel.
Blue−Eye Mold−Damaged Kernels (corn)	Kernels with blue mold in the germ. Blue−eye mold should not be confused with purple plumule, which is not a type of damage. Purple plumule is generally purple in color and is always found in the center of the germ.
Cob Rot−Damaged Kernels (corn)	Kernels that are distinctly discolored or rotting as a result of a fungus that attacks corn ears.
Drier−Damaged Kernels	Kernels that are discolored, wrinkled, and blistered; or are puffed or swollen and slightly discolored, and often have damaged germs; or whose seed coats are peeling off or appear fractured.
Frost−Damaged Kernels	Kernels that are discolored, blistered, or have a slightly flaked−off bran coat; or kernels with a distinctly wax−like or candied appearance due to frost.
Germ−Damaged Kernels	Kernels that are discolored by heat or mold resulting from respiration.
Ground− or Weather−Damaged Kernels	Kernels with dark stains or discoloration and rough cake−like appearance caused by ground and/or weather conditions.
Heat−Damaged Kernels	Kernels that are materially discolored and damaged by external heat or as the result of heating caused by fermentation.
Immature− or Green−Damaged Kernels	Kernels that are intensely green in color.
Malt−Damaged Kernels (barley)	Kernels that have undergone the malting process and show any degree of sprout.
Mold−Damaged Kernels (External)	Kernels that have **considerable** evidence of mold.
Mold−Damaged Kernels (Internal)	Kernels that have **any** evidence of mold.
Scab−Damaged Wheat Kernels	Kernels having a dull, lifeless, and chalky appearance.
Weevil− or Insect−Damaged Kernels	Kernels which bear evidence of boring or tunneling by insects.

The Official United States Standards for Grain describe the numerical grades for cereals (barley, oats, rye, triticale, wheat, etc.). The lowest grade that may be assigned to any of these grains is "U.S. Sample grade." This grade is applied to grain that:

- Does not come within the grade requirements of any of the numerical grades;
- Has a musty, sour, or commercially objectionable foreign odor;
- Is heating;
- Contains 32 or more insect−damaged kernels per 100 grams (wheat only);
- Is contaminated with stones, pieces of glass, toxic seeds, unknown or toxic substances, animal filth, crotalaria seeds, or castor beans;
- Is otherwise of distinctly low quality.

Table 5: Grade classes for wheat in the United States

U.S. Grade	No.1	No.2	No.3	No.4	No.5
	Minimum pound limits of −−				
TEST WEIGHT (lbs/bu)					
Hard Red Spring wheat or White Club wheat	58.0	57.0	55.0	53.0	50.0
All other classes and subclasses	60.0	58.0	56.0	54.0	51.0
	Maximum limits of −−				
DEFECTS					
Damaged kernels					
−−Heat (part of total)	0.2	0.2	0.5	1.0	3.0
−−Total	2.0	4.0	7.0	10.0	15.0
Foreign material	0.4	0.7	1.3	3.0	5.0
Shrunken and broken kernels	3.0	5.0	8.0	12.0	20.0
Total*	3.0	5.0	8.0	12.0	20.0
WHEAT OF OTHER CLASSES**					
Contrasting Classes	1.0	2.0	3.0	10.0	10.0
Total***	3.0	5.0	10.0	10.0	10.0
STONES	0.1	0.1	0.1	0.1	0.1
	Maximum count limits of −−				
OTHER MATERIAL					
Animal filth	1	1	1	1	1
Castor beans	1	1	1	1	1
Crotalaria seeds	2	2	2	2	2
Glass	0	0	0	0	0
Stones	3	3	3	3	3
Unknown foreign substance	3	3	3	3	3
Total****	4	4	4	4	4
INSECT−DAMAGED KERNELS IN 100 GRAMS	31	31	31	31	31

In Table 5:

*Includes damaged kernels (total), foreign material, and shrunken and broken kernels.

**Unclassed wheat of any grade may contain not more than 10.0 percent of wheat of other classes.

***Includes contrasting classes

****Includes any combination of animal filth, castor beans, crotalaria seeds, glass, stones, or unknown foreign substance.

2.1.3. Regulation of standard qualities for common wheat, rye, barley, maize and durum wheat in the European Community

The regulation EEC No. 2731/75 of the Council of 29 October 1975 is to fix standard quality and price for wheat, rye, maize, sorghum and durum wheat with reference to specific standard qualities. These specifications should correspond as far as possible to the average qualities of those cereals harvested under normal conditions within the community. This document was modified more times. The last amendment was done by document 397R2594, in 1997.

The standard quality for which the target price and the threshold prices for common wheat are fixed is defined as wheat of a sound and fair merchantable quality, free from abnormal smell and live pests, of a color specific to this cereal (*article 1*). The physical quality criteria:

- moisture content should not exceed 14 %.
- The total percentage of matter other than basic cereals of unimpaired quality is maximum 5 %, of which the maximum percentage of
  - broken grains is 2 %
  - grain impurities is 1.5 %. This means shriveled grains, grains of other cereals, grains damaged by pests, grains showing discoloration of the germ and grains heated by drying.
  - sprouted grains is 1 %
  - miscellaneous impurities is 0.5 %. This group consists of extraneous seeds, damaged grains, extraneous matter, husks, ergot, decayed grains, dead insects and fragments of insects.

The specific weight is 76 kg/hl. The technical quality criteria for common wheat are:

- the dough from such wheat does not stick during the mechanical kneading process
- the protein content (5.7 x N), in terms of dry matter, is at least 11.5 %
- the Zeleny index is at least 25
- the Hagberg falling number is at least 230, including preparation (agitation) time of 60 s

The standard quality for rye is defined as rye of a sound and fair marketable quality, free from abnormal smell and live pests, of a color proper to this cereal (*article 2*). Maximal moisture content is 16 %. The total percentage of matter other than basic cereals of unimpaired quality is maximum 5 %, of which the maximum percentage of

- broken grains is 2 %
- grain impurities is 1.75 %. Impurities means shriveled grains, grains of other cereals, grains damaged by pests and grains overheated during drying.
- sprouted grains is 1 %
- miscellaneous impurities is 0.5 %. Miscellaneous impurities consist of extraneous seeds, damaged grains, extraneous matter, husks, ergot, dead insects and fragments of insects.

Specific weight of rye is 71 kg/hl.

The standard quality for barley means barley of a sound and fair marketable quality, free from abnormal smell and live pests, of a color proper to this cereal (*article 3*). Maximal moisture content is 16 %. The total percentage of matter other than basic cereals of unimpaired quality is maximum 6 %, of which the maximum percentage of

- broken grains is 2 %
- grain impurities is 2 %, where impurity means shriveled grains, grains of other cereals, grains damaged by pests and grains overheated during drying.
- sprouted grains is 1 %
- miscellaneous impurities is 1 %. The group of miscellaneous impurities consists of extraneous seeds, damaged grains, extraneous matter, husks, dead insects and fragments of insects.

Standard specific weight for barley is 67 kg/hl.

The standard quality for which the target price, the intervention price and the threshold price for maize are fixed is defined as maize of a sound and fair marketable quality, free from abnormal smell and live pests (*article 4*). The allowed maximum moisture content is 15.5 %. The total percentage of matter other than basic cereals of unimpaired quality is maximum 8 %, of which the maximum percentage of

- broken grains is 2 %, where broken grains mean pieces of grain or grains which pass through a sieve with a circular mesh 4.5 mm in diameter.
- grain impurities is 4 %. This means grains of other cereals, grains damaged by pests and grains heated by drying.
- sprouted grains is 1 %
- miscellaneous impurities is 1 %. This group consists of extraneous seeds, damaged grains, extraneous matter, cob fragments, dead insects and fragments of insects.

The standard physical quality criteria for durum wheat is defined as durum wheat of a sound, genuine and fair merchantable quality, free from abnormal smell and live pests, amber yellow to brown in color, with a vitreous section of translucent, horny appearance (*article 5*). Maximal moisture content is 13 %. Total percentage of matter other than durum wheat grains of unimpaired quality is maximum 25 %, of which the maximum percentage of

- durum wheat grains which have wholly or partly lost their vitreous aspect is 20 %
- broken grains is 2 %
- grain impurities is 2 %. Shriveled grains, grains of other cereals, grains damaged by pests, grains showing discoloration of the germ, mottled grains, grains affected with fusariosis and grains overheated during drying are selected.
- sprouted grains is 0.5 %
- miscellaneous impurities is 0.5 %, where it means extraneous seeds, damaged grains, extraneous matter, husks, ergot, decayed grains, dead insects and fragments of insects.

Specific weight for durum wheat is 80 kg/hl. Technology quality criteria:

- protein content (5.7 x N) is not less than 12.5 % of dry matter
- gluten content is not less than 8.75 % of dry matter
- Hagberg falling number is not less than 250, including 60 s preparation (agitation) time

According to the regulation of European Community

- all grains of which endosperm is partially uncovered shall be considered as broken grains. Grains damaged by threshing and grains from which the germ has been removed also belong to this group. This definition does not apply to maize.
- grains which, after elimination of all other matter, pass through sieves with apertures of 2 mm for wheat, 1.8 mm for rye, 1.9 mm for durum wheat or 2.2 mm for barley shall be considered as shriveled grains. In addition, grains damaged by frost and unripe (green) grains belong to this group.
- other cereals in grain impurities means all grains which do not belong to the species of grain sampled.
- extraneous seeds are seeds of plants, whether or not cultivated, other than cereals. They include seeds not worth recovering, seeds which can be used for livestock and noxious seeds. Noxious seeds means seeds which are toxic to humans and animals, seeds hampering or complicating the cleaning and milling of cereals and seeds affecting the quality of products processed from cereals.
- grains overheated during drying are grains which show external signs of scorching but which are not damaged.
- grains damaged by pests are those which have been nibbled or insect−bored.
- grains showing discoloration of the germ are those of which the tegument is colored brown to brownish black and of which the germ is normal and not sprouting. For common wheat, grains showing discoloration of the germ are disregarded up to 8 %. For durum wheat, mottled grains are grains which show brown to brownish black discoloration on parts other than the germ and grains affected with fusariosis are grains whose pericarp is contaminated

with *Fusarium* mycelium. *Fusarium* attacked grains look slightly shriveled, wrinkled and have pink or white diffuse patches with an ill−defined outline.

- sprouted grains are those in which the radicle or plumule is clearly visible to the naked eye. However, account must be taken of the general appearance of the sample when its content, of sprouted grains is assessed. In some kinds of cereals the germ is protuberant (e.g. durum wheat) and its tegument splits when the batch of cereals is shaken. These grains resemble sprouted grains but must not be included in that group. Sprouted grains are only those where the germ has undergone clearly visible changes which make it easy to distinguish the sprouted grain from the normal.
- damaged grains are those rendered unfit for human consumption and, as regards feed grain, for consumption by cattle, owing to putrefaction, mildew, bacterial or other causes. Grains which have deteriorated through spontaneous generation of heat or by too extreme drying also belong to this group. These are fully grown grains in which the tegument is colored grayish brown to black, while the cross−section of the kernel is colored yellowish gray to brownish black. Grains attacked by wheat−midge shall be considered as damaged grains only when more than half the surface of the grain is colored gray to black as a result of secondary cryptogamic attack. Where discoloration covers less than half of the surface of grain, the latter must be classed with grains damaged by pests.
- mitadiné grains of durum wheat are grains whose kernel cannot be regarded as entirely vitreous.
- All matter in a sample of cereals retained a sieve with apertures of 3.5 mm (with the exception of grains of other cereals and particularly large grains of the basic cereal) and that passing through a sieve with apertures of 1 mm shall be considered as extraneous matter. Stones, sand, fragments of straw and other impurities in the sample which pass through a sieve with apertures of 3.5 mm and are retained by a sieve with apertures of 1 mm are also included in this group. This definition does not apply to maize. For that cereal, all matter in a sample which passes through a sieve with apertures of 1 mm must be considered as extraneous matter.

2.2. Digital imaging

2.2.1. Illumination

Computer vision is not limited to visible radiation. As soon as imaging detector systems became available, other types of radiation were used to probe scenes and objects of interest. Recent developments in imaging sensors cover almost the whole electromagnetic spectrum from x−rays to radiowaves. In standard applications, illumination is frequently taken as given and optimized to illuminate objects evenly with high contrast. Such setups are appropriate for object identification and geometric measurements. Monochromatic illumination consists of a certain frequency. The distribution of radiation over the range of possible wavelengths is called the spectrum or spectral distribution. Only a very narrow band of electromagnetic radiation between 380 nm and 780 nm is visible to the human eye. Light is received by stimulating the retina after passing the preretinal optics of eye. The retina consists of two different type of sensors: rods and cones. At high levels of irradiance the cones are used to detect light and to produce the sensation of colors (this is called *photopic vision*). Rods are used mainly for night vision at low illumination levels (this is called *scotopic vision*). The peak of the relative spectral luminous efficiency for scotopic vision can be found at 507 nm compared to the peak at 555 nm for photopic vision. As the response of the human eye to radiation depends on a variety of physiological parameters, differing for individual human observers, the spectral luminous efficiency can correspond only to an average normalized observer. At intermediate illumination levels both photopic and scotopic vision are involved. This range is called *mesopic vision*. (B. Jähne, H. Haußecker and P. Geißler, 1999, vol.1)

The most important properties of illumination sources are: spectral characteristics, intensity distribution, radiant efficiency, luminous efficacy, electrical properties, temporal characteristics and package dimensions. In many cases, features of interest can be made visible by a certain geometrical arrangement or spectral characteristics of the illumination rather than by trying to use expensive computer vision algorithms to solve the same task. Good image quality increases the performance and reliability of any processing algorithm. Single illumination sources are not the only way to illuminate the scene. For outdoor scenes, natural sources, such as solar irradiance and diffuse sky irradiance, play an important role. In some applications, they might be the only illumination sources available. In other cases, they are unwanted sources of errors and they have to be eliminated. In order to acquire images of good quality, artificial illumination sources are used:

- incandescent lamps are among the most popular all−purpose illumination sources. The most prominent examples are standard light bulbs with carbon or tungsten (more modern version) filament.
- discharge lamps operate on the physical principle of gas discharge. *Spectral lamps* are plain gas discharge lamps, without additional coatings, filled with xenon (Xe), mercury (Hg) or their mixtures. *Fluorescent lamps* are discharge lamps (usually filled with Hg) that are additionally coated with special fluorescent materials. These layers absorb ultraviolet radiation and convert it into longer wavelength radiation in the visible region, which is finally emitted.
- arc lamps have anodes and cathodes made of tungsten and sealed in clear quartz glass (filled with deuterium, Hg or Xe−Hg mixture).
- infrared emitters are emitters of thermal radiation from quartz tungsten halogen lamps to lamps with high ohmic resistance.
- Light−emitting diodes (LEDs) are small and powerful light sources. Their most important advantages are: high luminous efficacy, small dimensions, suitability for integration into large arrays of any arbitrar shape, low power consumption, and fast response time.
- lasers are the most powerful monochromatic light source available. Lasers usually have low radiant efficiency and high luminous efficacy. Lasers are available for a large variety of spectral ranges, from x−rays into the microwave region.

According to the position of artificial light sources, the following setups are distinguished:

- directional illumination or specular illumination denotes a setup in which parallel light or light from a point light source is used to illuminate the object. This is the most simple type of illumination, consisting of single light sources at a certain distance from the surface of object.
- diffuse illumination consists of an extended source, which emits light in all directions. Examples are extended diffusing plates, rings, and fiber optical illumination.
- rear illumination is used if the geometrical outline of a flat object is of interest.
- bright field illumination, where a direct path exists from the light source to the camera. As long as no object present, the image appears bright.
- telecentric illumination is used to convert the spatial radiance distribution of a light source into bundles of parallel rays that reflect the radiance (and spectral distribution) of a single point of the light source.
- pulsed illumination can be used to increase the performance of the illumination system, reduce blurring effects, measure time constants and distances, and allow fast image processing.

2.2.2. Color measurement

Commission Internationale de l'Éclairage (CIE) is the international organization that undertook the task of developing specifications for colorimetry. The CIE standard colorimetry is based on a trichromatic system of red, green, and blue color components (with peaks at 700 nm, 546.1 nm, and 435.8 nm respectively). A color matching function is used to compute color from R,G,B signals:

$$C(\lambda) = R \cdot [R] + G \cdot [G] + B \cdot [B] \qquad \text{(Eq.1)}$$

this C(λ) represents only the color information. Luminance of a color matched by the amounts *R* red units, *G* green units and *B* blue units will be (Schanda, 2000):

$$L = 1.0000 \cdot R + 4.5907 \cdot G + 0.601 \cdot B \qquad \text{(Eq.2)}$$

If R, G and B values are computed from radiometric quantities, L will be the corresponding photometric quantity. There are negative values in the original colour space of RGB signals that may lead to computation errors. For this reason this space is transformed into the X,Y,Z colour space. The basis vector transformation was done in such a form that

1. the tristimulus values of the colour stimulus of the equi−energetic spectrum should again be equal;
2. all the photometric information (luminance, if the stimulus is measured in radiance units) should be presented in a single parameter;
3. the tristimulus values of all real colours should be positive and the volume of the tetrahedron should be as small as possible (i.e. the borders of the colour cone should touch the tetrahedron at as many as possible places).

Color matching functions can be built in this system, as well (Fig.1.). Using these functions, the *X*, *Y*, *Z* tristimulus values of a colour stimulus (S(λ)) can be calculated. The colour stimulus distributions are presented in Fig.2. Color matching and stimulus functions are presented on the basis of data tables published in CIE 1931 Standard Colorimetric Observer.

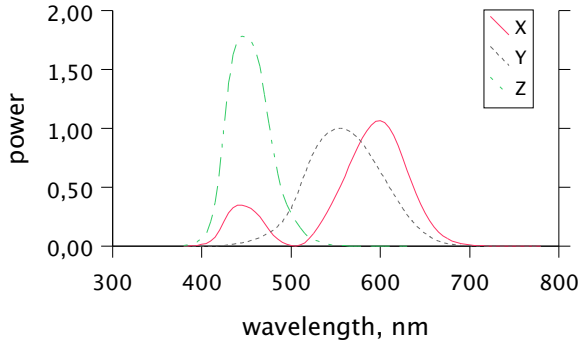

Fig.1: X,Y,Z color matching functions

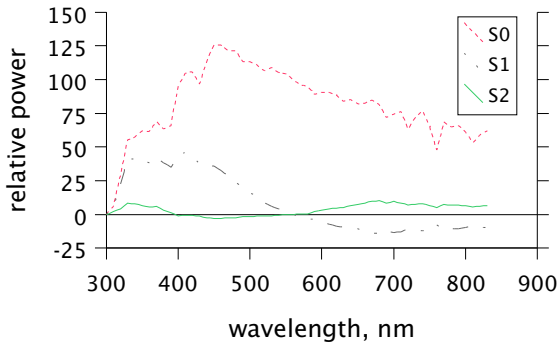

Fig.2: Color stimulus functions

Unfortunately the *X*, *Y*, *Z* tristimulus values are not very easy to interpret and it is not very easy to "see" the color they specify. As the luminance measure has been condensed into the *Y* tristimulus value, it seemed to be reasonable to transform from the *X*, *Y*, *Z* space into another space where *Y* is one of the coordinates and the other two are describing chromaticity. To do this the CIE introduced the chromaticity coordinates *x*, *y*, *z* and defined them in the following form:

$$x=\frac{X}{X+Y+Z};y=\frac{Y}{X+Y+Z};z=\frac{Z}{X+Y+Z} \qquad \text{(Eq.3)}$$

As $x + y + z = 1$, it is enough to use two of the chromaticity coordinates to describe the chromaticity of the stimulus. It is usual to use *x* and *y*, and to plot the chromaticities in a *chromaticity diagram*.

As the reflection properties of average samples might differ considerably from those of an ideal standard, i.e. they are neither totally diffuse (Lambertian) nor are they reflecting only regularly (mirror like), at different locations and with different instruments reproducible measurements can only be achieved if the measuring geometry used is the same. The CIE standardized four measuring geometries: 45°/normal, normal/45°, diffuse/normal and normal/diffuse. Here the first angle description refers to irradiation, the second to observation (Lukács, 1982; Schanda, 2000):

Case a) 45°/normal (symbol: 45/0): The specimen is irradiated by one or more beams whose effective axes are at an angle of 45°±2° from the normal to the specimen surface. The angle between the direction of viewing and the normal to the specimen should not exceed 10°. The angle between the axis and any ray of an irradiating beam should not exceed 8°. The same restriction should be observed in the viewing beam.

Case b) normal/45°(symbol: 0/45): The specimen is irradiated by a beam whose effective axis is at an angle not exceeding 10° from the normal to the specimen surface. The specimen is viewed at an angle of 45°±2° from the normal to the specimen surface. The angle between the axis and any ray of the irradiating beam should not exceed 8°. The same restriction should be observed in the viewing beam.

Case c) diffuse/normal (symbol d/n): The specimen is irradiated diffusely by an integrating sphere. The angle between the normal to the specimen surface and the axis of the viewing beam should not exceed 10°. The integrating sphere may be of any diameter provided the total area of the ports does not exceed 10 percent of the internal reflecting sphere area. The angle between the axis and any ray of the viewing beam should not exceed 5°.

Case d) normal/diffuse (symbol: 0/d): The specimen is irradiated by a beam whose axis is at an angle not exceeding 10° from the normal to the specimen surface. The reflected flux is collected by means of an integrating sphere. The angle between the axis and any ray of the irradiating beam should not exceed 5°. The integrating sphere may be of any diameter provided the total area of the ports does not exceed 10 percent of the internal reflecting sphere area.

For the conditions ’diffuse/normal’ and ’normal/diffuse’ the regularly reflected component of specimens with mixed reflection may be excluded by the use of a gloss trap. If a gloss trap is used, details of its size, shape and position should be given.
In the ’normal/diffuse’ condition the sample should not be measured with a strictly normal axis of irradiation if it is required to include the regular component of reflection. Similarly, in the ’diffuse/normal’ condition the sample should not be measured with a strictly normal axis of view if it is required to include the regular component of reflection.
Case a), b) and c) give values of reflectance factor, $R(\lambda)$. For directional viewing with a sufficiently small angular spread, these reflectance factors become identical to radiance factors. For case d), viewing with an integrating sphere, in ideal case the reflectance is measured.

Fig.3: Computer generated color spectra

Computers represent color with the mixture of red, green and blue color components. Intensity values are scaled from 0 to 255 (limits of one byte). Each point of the picture (called *pixel*) has its own R, G and B values in the case of 24 bit/pixel color depth. Figure 3 presents available colors for computers. Besides color information, coefficients contain intensity of pixels, as well. In order to compute independent color information, normalization can be used. Simple (case a) and quadratic (case b) normalization are introduced in Eq.4. After this step all color vectors have the same length and are comparable with less dependence on illumination.

$$\text{a.)}\quad r=\frac{R}{R+G+B}\qquad \text{b.)}\quad r=\frac{R^2}{R^2+G^2+B^2} \tag{Eq.4.}$$

Red, green and blue intensity values are usually transformed into the hue−saturation−intensity (HSI) system (or HSV, where V = value). This is called the Munsell color system. The transformation between HSI and RGB color spaces is presented in Eq.5 (Majumdar, Jayas, 2000). Value represents the brightness or total intensity, degree of saturation (or chroma) means how muted or vivid the color is, and correspondence to the dominant wavelength is called hue (Fig.4). The chief advantage of such systems is that color is split into conceptually distinct parts This distinction cannot be made within the RGB system (Ewing, Horton, 1999).

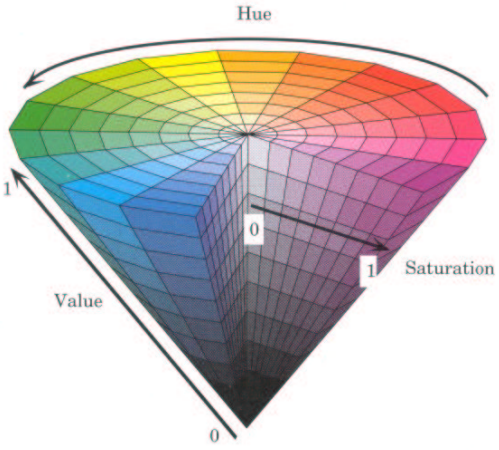

Fig.4: HSI color system (MathWorks)

$$I=\frac{R+G+B}{3}\qquad S=1-\frac{min(R,G,B)}{I}$$

$$H=\cos^{-1}\left\{\frac{\frac{1}{2}[(R-G)+(R-B)]}{[(R-G)^2+(R-B)(G-B)]^{1/2}}\right\}\quad \text{where if}\quad \frac{B}{I}>\frac{G}{I}\quad \text{then } H=360^{o}-H \tag{Eq.5}$$

Majumdar and Jayas (2000) used red, green, blue, hue, saturation and intensity parameters with their average value, range and variance. Ranking of color features of individual kernels (independently) is presented in Table 6. Red, green and blue average values are at the top of the table. Intensity, saturation and hue reached lower positions.

Table 6: Ranking of color features with STEPDISC analysis (n=31500)

No.	Color features of individual kernels	Average squared canonical correlation	r^2
1	Red	0.112	0.49
2	Green	0.115	0.46
3	Saturation range	0.105	0.42
4	Intensity	0.103	0.41
5	Blue	0.080	0.32
6	Saturation	0.078	0.31
7	Red range	0.067	0.27
8	Green range	0.067	0.27
9	Intensity range	0.057	0.23
10	Hue	0.054	0.22
11	Saturation variance	0.047	0.19
12	Blue variance	0.045	0.18
13	Green variance	0.038	0.15
14	Intensity variance	0.037	0.15
15	Blue range	0.036	0.15
16	Red variance	0.031	0.12
17	Hue variance	0.025	0.10
18	Hue range	0.008	0.03

The red−, white− and amber−colored wheat classes were well separated in Canada, according to their mean RGB reflectance properties (Neuman *et.al.*, 1989, I−II.). Discrimination of red spring classes was relatively high (above 90%), but classification of varieties within these groups was not successful.

According to the current trends in digital image analysis, average RGB values are usually augmented with surface color distribution parameters. J. Meuleman and C. van Kaam used unsupervised neural networks in 1997, in order to improve segmentation of leaves, flowers, stamen, stems and background. Eighteen parameters were used to feed the neural network: red, green and blue intensities of the selected pixel, normalized RGB values of the same pixel, and normalized RGB values of four additional pixels in the 5x5 environment of the central point. Three layers partitioned input data set into two subsets recursively. Classification was evaluated in each step on the basis of deviation of new classes compared to the original set. The partitioning process was stopped if the following ratio became too low:

$$\frac{\sum (n_1 \cdot X_{1,i}^2 + n_2 \cdot X_{2,i}^2)}{\sum \sum (x_{1,i,j} - X_{1,i})^2 + \sum \sum (x_{2,i,j} - X_{2,i})^2} \qquad \text{(Eq.6)}$$

where n_1 and n_2 mean the number of pixels, x the intensity parameters, X the average values. This clustering approach on a 450−pattern data set made only one mistake: one pixel of stamen was recognized as leaf.

2.2.3 Shape estimation

Digital images are data matrices, where each element of the matrix contains color information about the represented area of the real scene. Comparison of these values allows computers to distinguish between foreground and background parts of the picture and to select objects. The shape of the selected area may be estimated several ways according to the purpose of analysis. These methods are based on the coordinates of the pixels belonging to the object of interest.

In the work of Marshall, Ellison and Mares (1984; 1986) simple geometric models of wheat grains were analyzed to determine the effects of changes in shape and size on volume per unit surface area and hence potential milling yield. The shape and size of kernels of Australian cultivars were measured and found to be significantly different from the optimum required to maximize volume per unit surface area (spherical shape). For kernels of a given mean volume, the questions of concern to the plant breeder interested in improving milling yield by altering kernel shape and size are:

- What are the optimum dimensions of a kernel (length, width and height) so that grain volume per unit surface area and milling yield are maximized?
- Is the potential increase in milling yield that can be achieved by altering kernel dimensions large enough to justify selection for optimum grain shape in breeding programs?
- Is there sufficient variability in wheat germplasm to develop varieties with optimum grain shape?

Similarly, for kernels of a given shape and dimensions the critical questions are:

- What is the relationship between volume per unit surface area and grain volume?
- How large an increase in kernel volume would be required to significantly improve milling yield in wheat?
- Is there sufficient genetic variability among bread wheat and their near relatives to achieve such an increase in kernel volume?

To answer the first question, five geometric models were examined: cylinder, rectangular prism, triangular prism, double cone and prolate spheroid. These unrealistic models were used to factor out the best way of improvement of milling yield (Fig.5).

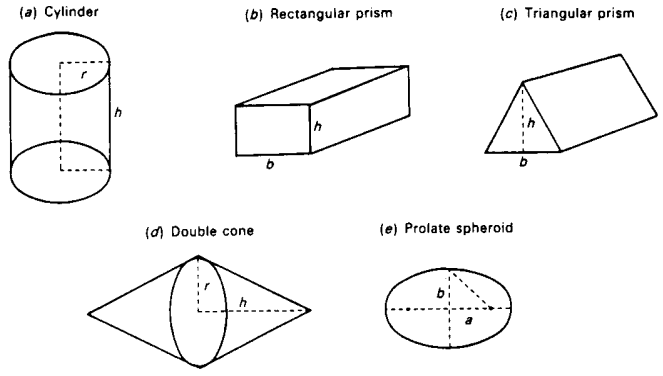

Fig.5: Five geometric models used by Marshall, Ellison and Mares in 1984

Increases in seed weight and volume are usually due more to increases in seed length than in seed width or height. For this reason, as grain volume is increased, there will be a correlated change in grain shape away from the optimum required to maximize volume per unit surface area of the seed.

Table 7: Parameters of some cultivated wheat varieties in Australia

variety or accession	length (*l*, mm)	width (*w*, mm)	height (*h*, mm)	*w/l*	*h/l*	100 grain weight (g)	volume (mm^3)
T. sphaerococcum							
AUS 3876	4.4	2.7	2.6	0.61	0.60	−−	−−
AUS 1201	4.4	2.5	2.9	0.57	0.65	−−	−−
AUS 1906	4.2	2.5	2.6	0.60	0.62	−−	−−
SA 14	4.5	2.9	3.1	0.67	0.66	2.98	21.8
SA 79	4.7	3.1	3.1	0.65	0.67	2.78	21.8
T. aestivum							
Spica	6.4	3.3	3.1	0.51	0.47	4.52	33.1
Glenlea	7.2	3.3	2.9	0.46	0.41	4.53	33.3
Pitic 62	6.6	2.7	2.6	0.40	0.39	3.17	23.9
Glenwari	6.4	3.3	3.1	0.51	0.48	4.61	33.7
Bluebird 4	6.3	3.3	2.9	0.53	0.47	4.25	31.1
Ford	6.5	3.2	2.8	0.49	0.43	3.98	30.2
Festival	5.2	3.1	3.2	0.59	0.61	3.57	26.1
Windebri	5.3	3.2	3.1	0.60	0.58	3.73	27.5
Winglen	5.7	3.2	2.9	0.57	0.51	3.48	25.6
Charter	5.6	3.2	3.1	0.57	0.55	3.52	25.7
Najah	7.5	3.7	3.3	0.49	0.44	6.72	48.3

Zayas, Pomeranz and Lai in 1989 used more sophisticated morphological parameters. They selected basic parameters (area, perimeter, length, width, Feret's diameters at 0°, 45°, 90° and 135°) and derivative parameters to create wheat pattern prototypes.

Table 8: Derived shape factors (Zayas, Pomeranz, Lai 1989)

Parameter	minimum	maximum
Area (pixels)	1000	21000
$Radius_{area}/radius_{perimeter}$	0.6	0.9
Perimeter/convex perimeter	1	1.3
Convex perimeter/length	2	2.5
Feret 0°/Feret 45°	0.4	0.7
Feret 90°/Feret 135°	1.1	1.4

The first parameter differentiates in size, the second one in concavity. The rest of parameters differentiate among objects with different degrees of symmetry. Table 9 shows the identity and number of wheat and non−wheat objects identified by multivariate discriminant analysis.

Table 9: Classification result (Zayas, Pomeranz, Lai 1989)

Object	No.	Wheat	Non−wheat
Without stones (test data)			
Wheat	34	33	1
Non−wheat	99	12	87
With stones (test data)			
Wheat	34	33	1
Non−wheat	158	23	135

Morphological and crush−force parameters were combined to identify six classes and seventeen varieties of wheat kernels by Zayas, Martin, Steele and Katsevich (1996). Although shape was measured from down and profile views with 26 attributes, only hard and soft wheat classes were discriminated.

Shatadal, Jayas, Hehn and Bulley in 1995 classified various seed types into primary grain, small seed and large seed categories. The seed types used in each category were: hard red spring wheat (HRS) and barley as primary grains; canola, brown mustard, yellow mustard, oriental mustard and flaxseed as small seeds; *Laird* lentils, *Eston* lentils, pea beans, green peas, black beans and buckwheat as large seeds. The objective of their study was to assess the classification success in identifying HRS wheat and barley from other small and large seeds using morphological features. Orientation of the kernels for camera viewing was random. The following parameters were measured: perimeter, area, width, maximum and minimum radii. The calculated parameters were: rectangular aspect ratio (ratio of length to width), thinness ratio (ratio of square of perimeter to area), radius ratio (ratio of maximum to minimum radii), area ratio (ratio of area to product of length and width) and H−ratio (ratio of mean to standard deviation of all radii). The result of classification is presented in Table 10.

Table 10: Correct recognition of seed categories (Shatadal *et al.*, 1995)

Categories	HRS wheat	Barley	Small seeds	Large seeds	N
HRS wheat	995	1	2	2	1001
Barley	4	995	0	0	999
Small seeds	0	0	4987	0	4987
Large seeds	28	3	0	5969	6000

Morimoto, Takeuchi, Miyata and Hashimoto (1998) measured the randomness of perimeter. They used chaotic parameters to detect irregular shapes. Attractors (Singh, Maru and Moharir, 1998; Bünner *et.al.*, 2000; Gleick, 2000) were drawn to show complexity of radial distances (radii) along the outline of objects. Let $R(i)$ be the radius of one point, where $i = 1 .. N$ and N is the length of perimeter. An attractor is drawn onto the plane with $X = R(i)$ and $Y = R(i+s)$ coordinates. The plane of $R(i)$ and $R(i+s)$ is called phase space. In case of a spherical shape, all radii are equal ($R(i)=R(j); i,j=1..N$), and its attractor is one single point. The more the shape differs from a sphere, the more complex its attractor will be. The complexity of the attractor depends on the value of shifts as well. If the shift is set to zero, all attractors are plotted on a line that starts at the origin and has a 45° slope. Morimoto *et al.* used variable shift and computed fractal dimensions (Eq.7). In Morimoto's work, attractors assumed the shape of ellipses and the ratio of widths of the smallest (W2) and the largest (W1) was calculated.

$$D = \frac{-\log L(\tau)}{\log \tau} \qquad \text{(Eq.7)}$$

where D means fractal dimension, $L(\tau)$ length of the total perimeter measured in τ (the length of basic step). Threshold values, in order to distinguish between good and badly shaped tomatoes, were from 0.375 to 0.531 for W2/W1 and from 1.464 to 1.514 for D.

Besides the measurement of chaotic properties, shapes can be compared to a template, an ideal shape profile (Liao *et.al.*, 1993; Firtha, 1998). A corn kernel profile was built by Liao *et.al.* in 1993 to identify broken kernels (Fig.6). Kernels were divided into three regions: crown, body and tip cap. Eight morphological features were extracted and analyzed with a neural network. This method reached 93.25% accuracy with round kernels and 97.5% with flat kernels, compared to human inspector classification. Firtha (1998) divided the outlines of onions into six regions and estimated them with mathematical functions (constant, exponential and cosine). The coefficients contain all information required to reconstruct shape, to compare the shapes of different varieties or to build the three−dimensional model of this vegetable. Martinovich and Felföldi (1996) used Fast Fourier Transform (FFT), the direct comparison of outlines and the Polar Qualification System (PQS) to evaluate shapes of onion varieties. The Polar Qualification System is a general and powerful data reduction method rooted in the evaluation of near infrared spectra. The quality point of spectra, or any spectra like data set, is defined as the center of its polar spectrum (polar coordinate system, where radius is the function of spectral value and angle is a function of wavelength). Three approaches exist to compute coordinates of the quality point (Kaffka, Gyarmati, 1998). The *Point* method is introduced in Eq.8:

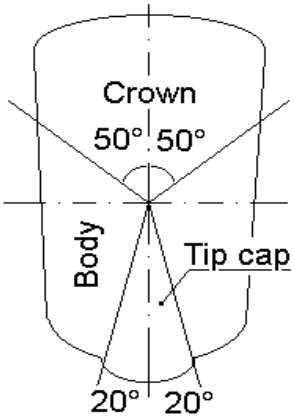

Fig.6: Corn shape model (Liao *et.al.* 1993)

$$x=\frac{1}{k}\sum_{i=0}^{k-1} V_{\lambda i}\cdot\cos(i\alpha) \qquad y=\frac{1}{k}\sum_{i=0}^{k-1} V_{\lambda i}\cdot\sin(i\alpha) \qquad \text{(Eq.8)}$$

The *Line* method is introduced in Eq.9:

$$x=\frac{1}{L}\sum_{i=0}^{k-1}\Delta L_i\cdot w_i \qquad y=\frac{1}{L}\sum_{i=0}^{k-1}\Delta L_i\cdot v_i \quad \text{, where}$$

$$\Delta L_i=\sqrt{(V_{\lambda(i+1)}\cos(i+1)\alpha-V_{\lambda i}\cos i\alpha)^2+(V_{\lambda(i+1)}\sin(i+1)\alpha-V_{\lambda i}\sin i\alpha)^2} \qquad \text{(Eq.9)}$$

$$w_i=\frac{V_{\lambda i}\cos i\alpha+V_{\lambda(i+1)}\cos(i+1)\alpha}{2} \qquad v_i=\frac{V_{\lambda i}\sin i\alpha+V_{\lambda(i+1)}\sin(i+1)\alpha}{2}$$

and L is the total length of the curve.

The *Surface* method is introduced in Eq.10:

$$x=\frac{1}{6T}\sum_{i=0}^{k-1}(v_{\lambda i}\cos i\alpha+V_{\lambda(i+1)}\cos(i+1)\alpha)\cdot V_{\lambda i}V_{\lambda(i+1)}\sin\alpha$$

$$y=\frac{1}{6T}\sum_{i=0}^{k-1}(v_{\lambda i}\sin i\alpha+V_{\lambda(i+1)}\sin(i+1)\alpha)\cdot V_{\lambda i}V_{\lambda(i+1)}\sin\alpha \qquad \text{(Eq.10)}$$

and $\quad T=\frac{1}{2}\sum_{i=0}^{k-1} V_{\lambda i}V_{\lambda(i+1)}\sin\alpha$, the area of the included surface.

These formulas calculate coordinates of quality points, where V_{li} is the spectral value, a = 360/k and k is the number of data points in the set (in our case it will be the length of perimeter in pixels).

Han, Feng and Weller in 1996 used two−dimensional Fourier transforms on enhanced images of corn kernels. Contrast was amplified and Roberts filter was used to enhance edges. Sixteen ring signatures, 16 wedge signatures and a DC value were used to describe each kernel. Two cultivars were tested and discriminant analysis was able to detect stress cracks with an average success ratio of 96.4% for Pioneer 3165 and 96.3% for Pioneer 3147.

2.2.4. Texture analysis

Texture is an important characteristic for the analysis of many types of images, from multispectral scanner images obtained from aircraft or satellite platforms to microscopic images of cell cultures or tissue samples. Despite its importance and ubiquity in image data, neither a formal approach nor a precise definition of texture exists. Texture discrimination techniques are for the most part ad hoc (Haralick, Shapiro 1992).

Statistical approaches use the autocorrelation function, the spectral power density function, frequency of edges per unit area, spatial gray level co−occurrence probabilities, gray level run−length distributions, relative extrema distributions, and mathematical morphology. An image texture is described by the number and types of its primitives and their spatial organization or layout. Gray level primitives are regions with gray level properties (average, minimum, maximum levels). A region is a maximally connected set of pixels having a certain gray level property. The spatial organization may be random, may have a pairwise dependence of one primitive on a neighboring primitive, or may have a dependence of *n* primitives at a time. This dependence may be structural, probabilistic, of functional (like a linear dependence).

The gray level spatial dependence approach characterizes texture by the co−occurrence of its gray levels. The gray level co−occurrence can be specified in a matrix of relative frequencies P_{ij}. Eight of the common features computed from this matrix are presented in Table 11, where *i* and *j* index variables mean the gray level (intensity of point in the gray−scaled image).

Table 11: Texture parameters (Haralick, Shapiro 1992)

Feature	Computation
Uniformity of energy	$\sum P_{i,j}^2$
Entropy	$-\sum P_{i,j} \cdot \log P_{i,j}$
Maximum probability	$\max(P_{i,j})$
Contrast	$\sum \lvert i-j \rvert^k (P_{i,j})^l$
Inverse difference moment	$\sum \frac{(P_{i,j})^l}{\lvert i-j \rvert^k}; i \neq j$
Correlation	$\sum \frac{(i-\mu)(j-\mu)P_{i,j}}{\sigma^2}$
where	$\mu = \sum i \cdot P_{i,j}$
Probability of a run length *n* for gray level *i*	$\sum \frac{(P_i - P_{i,j})^2 (P_{i,j})^{n-1}}{P_i^n}$
Homogeneity	$\sum \frac{P_{i,j}}{1+\lvert i-j \rvert}$
Cluster tendency	$\sum (i+j-2\mu)^k P_{i,j}$

The co−occurrence matrix is easy to understand and to compute quickly. If a vector is used instead of the co−occurrence matrix, the gray level difference spectrum is produced. Direction has significance because of the increased probability of dependence on texture position (rotation). Scanning direction and distance of compared pixels are defined by the displacement vector(s). In order to minimize dependence on the rotation of object, four directions are suggested: 0°, 45°, 90° and 135° (Jähne, Haußecker, Geißler, 1999, vol.2). As a result, the number of parameters is also increased.

Majumdar and Jayas (2000) tested the gray level co−occurrence matrix (GLCM) and gray level run length matrix (GLRM) based approaches. They concluded that the maximum number of gray levels in an image should be reduced from 256 to 8 to reduce computational time and increase accuracy. Fifteen parameters were used: 8 GLRM attributes, 4 GLCM attributes and 3 other (mean value, variance, range). These parameters were measured on individual color signals, gray level, and three color band combinations: G_1=(3R+2G+B)/6, G_2=(2R+G+3B)/6 and G_3=(R+3G+2B)/6. Classification accuracies were 92.0% (independent data sets) and 92.9% (test data sets).

Texture analysis techniques are very popular in remote sensing. The ages of tropical forest areas were estimated with fuzzy and texture−based processing and classification of Landsat images (Palubinskas *et.al.*, 1995). Eleven classes of regenerating forest were used to compare methods. Texture−based classifiers (based on a Markov random field model) consistently provided higher classification accuracy. Post−classification of fuzzy output was generally less accurate. The combination of Markov random field and neural networks was able to increase the effectiveness of segmentation or classification. Szirányi and Zerubia in 1997 used noisy artificial images (Fig.7) to measure the power of this combined method. The classification errors were 1.3% and 1.0% with the Modified Metropolis Dynamics and the Metropolis algorithm, respectively.

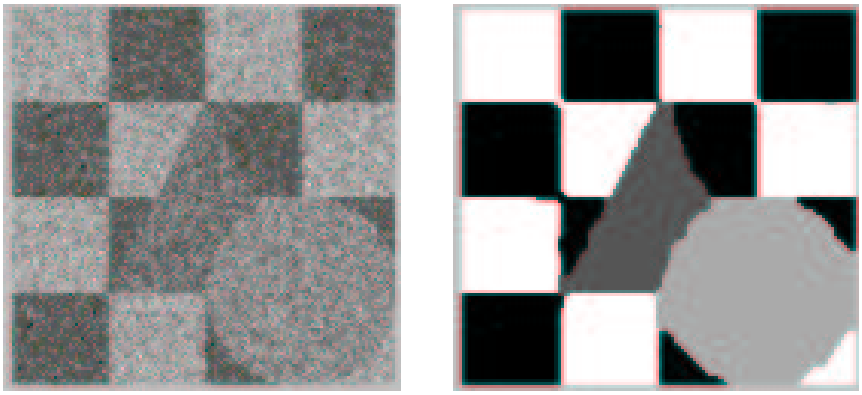

a.) b.)

Fig.7: Noisy image (a) and after segmentation (b)
(Szirányi, Zerubia, 1997)

2.3 Summary of literature

Current standards in Hungary, in the European Community and in the United States insist on measuring width and height of kernels to analyze shape, and human inspectors use handpicking in evaluation of the quality of grain samples. There are numerous applications for that purpose presented in the literature, but digital image processing offers more detailed analysis. Computer programs are able to acquire images of cereals (or fruits and vegetables) rapidly, and to calculate and evaluate parameters online.

Color can distinguish some types of seeds (wheat − brownish, corn − yellow or red, weed seeds and stones − gray) according to the intensity of red, green and blue color components. Because color is not enough to separate varieties within these classes, it is usually augmented with other visual attributes.

There are several approaches to model shapes of seed grains or fruits. Traditional parameters are width, height, and their ratio; average radius; area; and perimeter. There are ideal (expected) shapes, and they can be used as templates to fit to the objects. In this case, coefficients of template functions or shape factors are computed. In addition, chaotic properties are general factors to measure irregularity of shapes. If shapes are plotted into the phase space, their trajectories (attractors) will visualize chaos or irregularity as well.

Analysis of surface texture is hardly used in agriculture. A lot of methods were developed to process gray−scaled satellite images. They are very sophisticated and use the latest results of mathematical science. These techniques are able to segment areas of different surface structures, according to the periodic changes of shades and light parts. If these methods are extended to the color signals, color distributions or color patterns will be measured.

Accurate and objective measurement of visual parameters is able to complement other experiments (plant development, invention, optimization, etc.) with useful information.

3. Objectives

The objective of this work was to find visual quality parameters to measure shape, color and surface texture parameters of grains. The main goal was to combine these attributes so that computer programs would be able to distinguish different types of objects: wheat, string−pea, corn, barley, weed seeds, fragments of plants and fragments of insects.

In order to fulfill the objectives and understand the visual properties of objects, the following tasks were planned:

- segment the object and background parts of images with high accuracy, even if their intensities are close and they differ only in color (black background and dark brown weed seeds)
- model the shape of objects
  − with common mathematical functions (sine)
  − with polynomial functions
  − on the basis of regularity and self−similarity
- measure the average color of the surface with less dependence on illumination
- determine color distribution and texture of surface

4. Methods and materials

4.1. Vision system

The image acquisition system of the Department of Physics & Control at SzIE University was used. This setup is consisting of a Hitachi HV−C20 CCD camera, Canon zoom lenses, bulbs, grabber board (VIGA Window, AVER PCImager, Studio PCTV Pro) and a personal computer (Intel Celeron processor, 64 MB RAM). Three types of grabber boards were used, because of the hardware development of the system. A black tray was placed in front of the objective lens, approximately 4cm far away. On the basis of the CCD sensing area (7.95x6.45 mm), and the optical parameters of the lens system (focal length, distance of principal planes), dimensions of one pixel were approximately 0.055mm (width) and 0.055mm (height).

Only one object was placed on the tray at a time to capture as many details as possible. Images were stored in bitmap files with truecolor data format (24 bit/pixel). Depending on the grabber boards, 320x200 or 384x284 picture sizes were used.

4.2. Materials

Samples of wheat grains containing impurities were received from the milling industry, and wheat samples of known varieties were received from the National Institute for Quality Control in Agriculture (OMMI, Budapest). Table 12 presents the composition of the sample of seed grains and other materials. Numbers of grains in these parts represented their real occurrence.

Table 12: Composition of the sample

Name	Pieces	Percentage
Corn kernels	310	24.58
Barley kernels	209	16.57
Whole wheat grains	201	15.94
Small wheat grains	200	15.86
Broken wheat grains	56	4.44
Foreign materials*	57	4.52
Insect attacked wheat kernels	51	4.04
Mixture for testing, in which	177	14.04
− weed seeds	57	4.52
− fragments of plants	42	3.33
− broken wheat grains	37	2.93
− corn kernels	19	1.51
− string−pea	18	1.43
− stones	4	0.32
Total	1261	100.00%

*Materials passing through the first siever for wheat

Subgroups of this quantity were selected to teach and test the classification process. A special mixture (n=177, 14.04%) was separated to test the final version of the statistical evaluation and classification algorithm. The sample of whole wheat grains was divided into two groups: large and small grains. This division was done because whole wheat grains of small size are usually recognized incorrectly.

Fig.8: Foreign materials in the wheat sample

Extraneous seeds in the sample of wheat grains (Fig.8) were: string−pea, corn, barley and weed seeds. Besides these kernels, there were broken grains and stones as well. There were no noxious seeds in the sample.

4.3 Segmentation

The most important part of image processing is segmentation. This step discriminates background and object parts of the scene. The effectiveness of segmentation influences later processing such as shape recognition or color measurement.

The dynamic cluster algorithm was used to identify two classes of pixels. The objective of this algorithm is to find classes of extreme colors automatically. Segmentation was done in two steps. Initial cluster means were selected on the basis of 1% of the whole image in the first step (learning procedure). The total image was scanned in the second one and all pixels were classified into the nearest group and average values of color components (cluster means) were recalculated after each assignment. As a result of this process, there were two clusters separated as far as possible. Both of them were compared to the expected color of background and the closer one was eliminated from the image. The advantage of this method is that it is able to find classes of different colors with the same intensity.

A restoration algorithm was applied on the segmented image to add internal "background regions" to the object.

4.4 Shape description

4.4.1 Generating outline data sets

Points of the largest object were selected for further analysis, because only one object was placed onto the tray at the same time. The object has to be larger than 1000 pixels (approximately 3 mm^2), so that smaller particles can be ignored. Mass point − or gravity point − of the object was calculated and coordinates of perimeter pixels were stored in polar coordinates. Angle and distance − measured from the mass point − identify each point of the outline. Figure 9 presents sample shapes and the polar outlines.

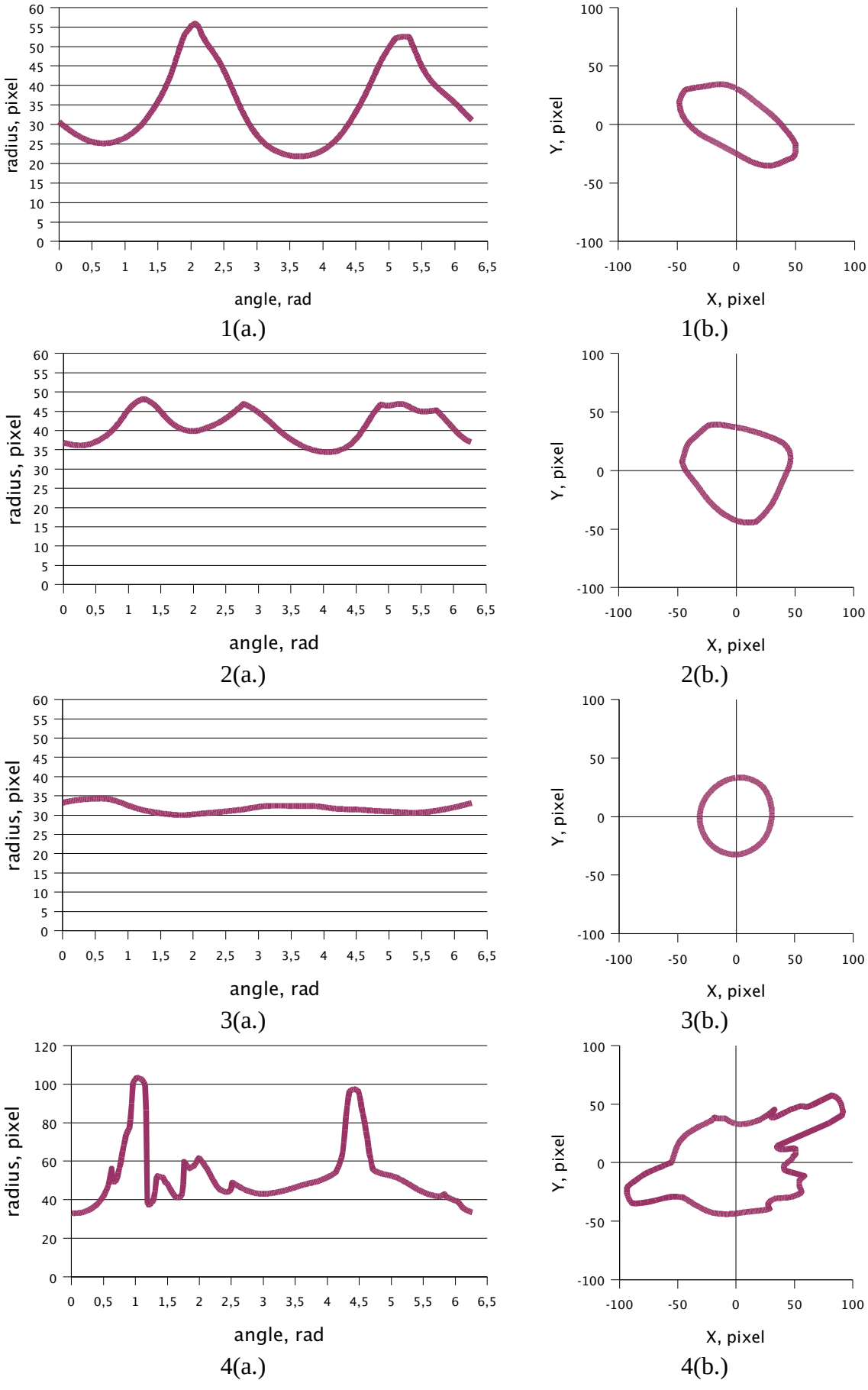

Fig.9: Polar data sets (a) and their real shapes (b): 1 − whole wheat kernel, 2 − corn, 3 − string−pea, 4 − fragment of plant

4.4.2 Estimation with mathematical functions

A stepwise optimization algorithm (Popper, Csizmás, 1993) was written to fit functions to the outline. It involved ten iterations and divided length of step by 2 in each cycle. As a result, it was able to estimate coefficients with an accuracy of ±0.1% of the initial values.

$$R = a + b \cdot \sin(c \cdot \alpha + d) \quad \text{(Eq.11)}$$

In case of Eq.11, an elliptic shape is assumed but the period of the sine function is variable. This makes the fitted curve able to estimate asymmetric shapes. However, the generated artificial shapes usually have a gap (Fig.10). Variables of Eq.11 have the following connotations:
a = average radius,
b = amplitude,
c = period of sine function,
d = rotation of object in front of the camera.

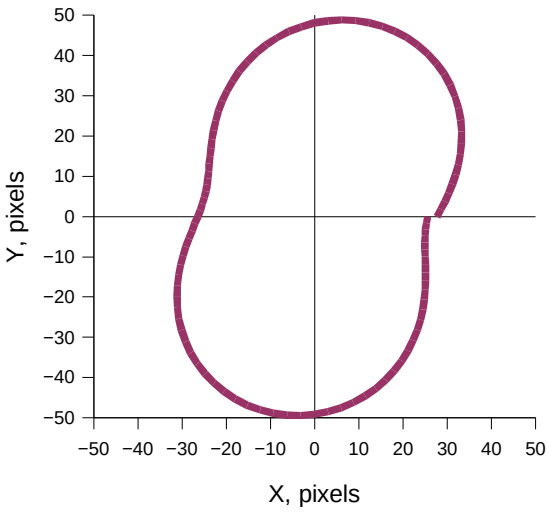

Fig.10: Estimated shape with Eq.11

$$R = a + (b + c \cdot \sin(\alpha + d)) \cdot \sin(2 \cdot \alpha + e) \quad \text{(Eq.12)}$$

Eq.12 uses an elliptic base with deformation. Figure 11 presents an example artificial outline of this function with the major axis of object and a line in the direction of deformation. This function is expected to estimate asymmetric figures of whole wheat kernels. Its variables are as follows:
a = average radius,
b = amplitude,
c = degree of deformation,
d = rotation of deformation,
e = rotation of object in front of the camera.

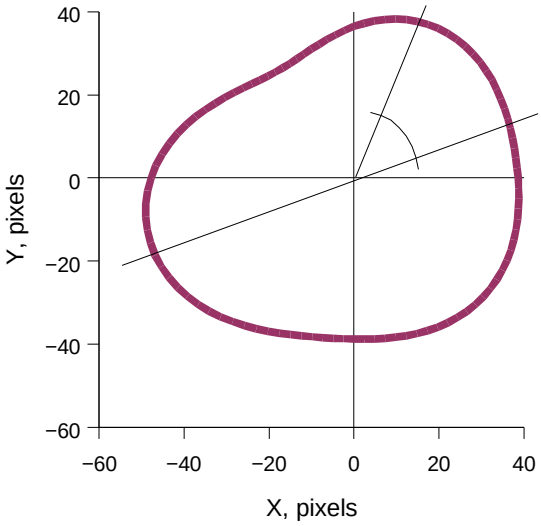

Fig.11: Estimated shape with Eq.12

A rational polynomial is introduced in Eq.13. This type of polynomial function obtained the highest correlation coefficient in the estimation of shape of whole wheat grains.

$$R = \frac{a + b \cdot \alpha + c \cdot \alpha^2 + d \cdot \alpha^3 + e \cdot \alpha^4}{1 + f \cdot \alpha + g \cdot \alpha^2 + h \cdot \alpha^3 + i \cdot \alpha^4} \quad \text{(Eq.13)}$$

Table 13 presents correlation coefficients for polynomial functions. Polynomial regression is very fast compared to the stepwise optimization methods and is able to fit more than two asymmetric peaks automatically.

Table 13: Average correlation coefficients for whole wheat grains

Value	Function
0.9770	$R=\frac{a+b\cdot\alpha+c\cdot\alpha^2+d\cdot\alpha^3+e\cdot\alpha^4}{1+f\cdot\alpha+g\cdot\alpha^2+h\cdot\alpha^3+i\cdot\alpha^4}$
0.9353	$R=a+b\cdot\alpha+c\cdot\alpha^2+d\cdot\alpha^3+e\cdot\alpha^4+f\cdot\alpha^5+g\cdot\alpha^6$
0.9028	$R=a+b\cdot\alpha+c\cdot\alpha^2+d\cdot\alpha^3+e\cdot\alpha^4+f\cdot\alpha^5+g\cdot\alpha^6+h\cdot\alpha^7$
0.8637	$R=a+b\cdot\alpha+c\cdot\alpha^2+d\cdot\alpha^3+e\cdot\alpha^4+f\cdot\alpha^5+g\cdot\alpha^6+h\cdot\alpha^7+i\cdot\alpha^8$
0.6663	$\frac{1}{R}=a+b\cdot\alpha+c\cdot\alpha^2+d\cdot\alpha^3+e\cdot\alpha^4+f\cdot\alpha^5$

Figure 11 presents how the sum of squares (error) decreased with increasing power of the polynomial. According to the analysis of variance of 2000 estimations (200 wheat grains in one cycle), the following powers were not different significantly:

- 7, 8, 9 and 10
- 6 and 7
- 4 and 5

Fig.11: Wheat shape estimation with polynomial regression

The problem in this case is that these types of mathematical functions are sensitive to the rotation of the data set (rotation of the object within the image) and they have oscillations at the very beginning and at the very end. In this case, this kind of oscillation can occur at 0° and 360° on the polar outline. In order to solve the problem of dependence on rotation and oscillation, the outline was shifted until the minimum radius was at 0°.

In the case of polynomial regression, there is no simple way to interpret coefficients (as it was possible with sine functions). A polynomial of power 8 has nine coefficients. There is an additional constant. Parameters were plotted as a polar diagram, where the angle identifies the coefficients and radii present their values. The quality point of this transformed curve and the area of its covering smallest rectangle were computed (Fig.12).

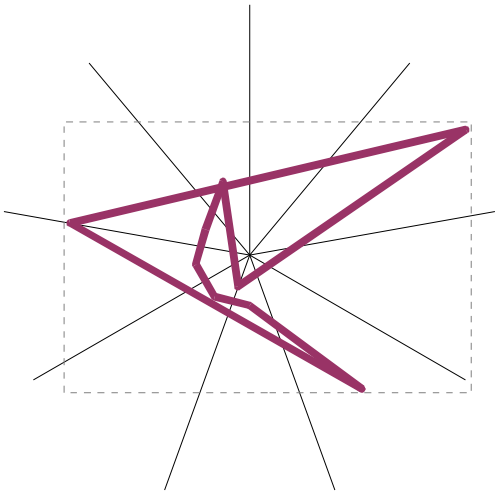

Fig.12: Quality profile diagram and evaluation of polynomial coefficients

4.4.3 Chaotic properties of shape

Chaos in shape means irregularity and complexity. Mathematical transformations were applied to reveal this attribute of polar outlines. Attractors (Singh, Maru, Moharir, 1998; Morimoto *et.al.*, 1998) were plotted and trajectories in the phase space were evaluated. This special function is called *attractor* in physical and mathematical sciences or *delay−function* in economics. It is derived from radii. One point on the phase space (in this case it is a plane) is identified by two radii with *d*, where *d* is the separation in pixels along the perimeter. Coordinates are R[i] and R[i+d]. When these radii are moved all along the whole perimeter, attractor will appear on the plane (Fig.13).

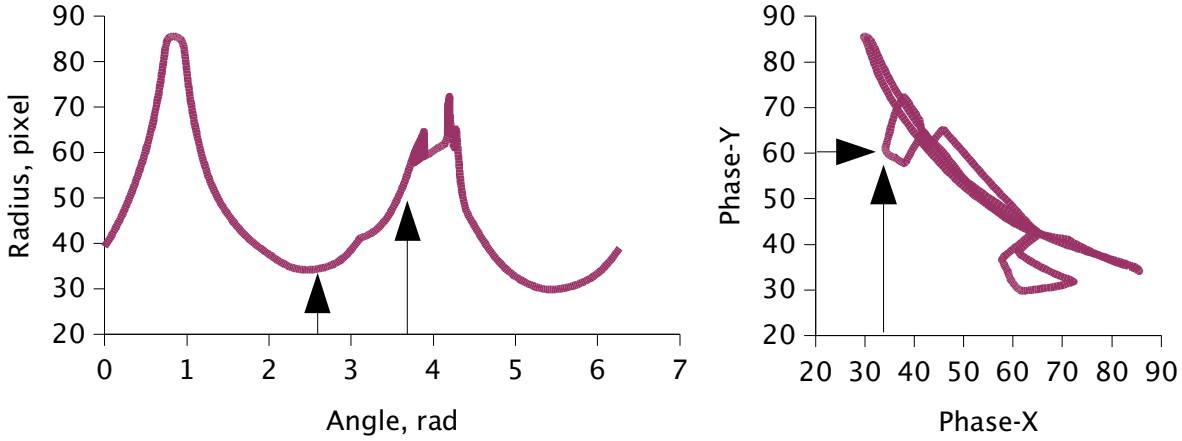

Normalized polar outline Attractor

Fig.13: Outline of a whole wheat grain and its attractor

If *d* is set to zero, all attractors are plotted along a line of slope 45°. Owing to the equal radii, spherical shapes have only one point, which is independent of *d*. In the present case, this distance was computed from the number of points in the perimeter: *d* = N/4. This 25% shift means approximately a 90° displacement of radii provided that the object is symmetric. Figure 14 presents sample of shapes and their attractors.

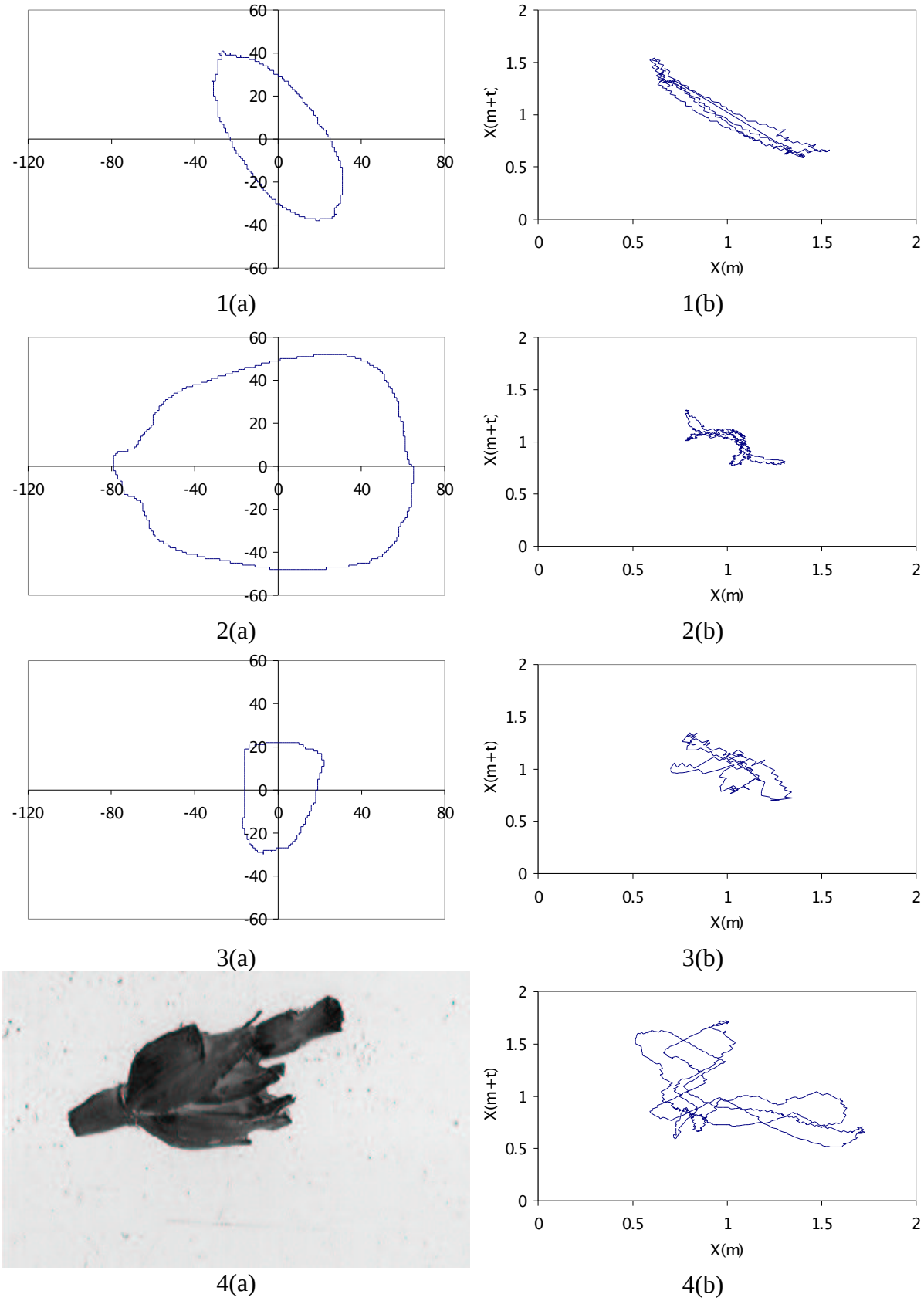

Fig.14: Objects (a) and their normalized attractors (b): 1 − whole wheat grain, 2 − corn, 3 − broken wheat kernel, 4 − fragment of plant

Evaluation of these curves was based on three attributes:

- area of the smallest covering square
- percentage of area of attractor within this square
- perimeter index

Perimeter index is defined as the number of perimeter pixels per unit area, dividing by the average radius (Eq.14). It is a type of density function.

$$PI = \frac{N}{\bar{R} \cdot (r_{max} - r_{min})^2} \qquad \text{(Eq.14)}$$

where: N − length of perimeter in pixels
R − radius
r − normalized radius

The area of the smallest covering square was divided into 400 identical squares with a 20x20 mesh. Cells containing points of the trajectory were counted to calculate the percentage of the smallest covering area of the attractor. Theoretically, the accuracy was ±0.125% .

Using the polar outline data, a 360x360 chaos map was generated, and evaluated according to their visible textures. The whole outline was compressed into a vector of 360 elements, where each item contained the average radius of the corresponding sector of shape (from 0° to 360°). The map visualizes differences of radii, as follows:

$$map(x,y) = \frac{|R(x) - R(y)|}{R_{max} - R_{min}} \quad ; \text{x=0..360}^{o} \text{ and y=0..360}^{o} \qquad \text{(Eq.15)}$$

This value is scaled between 0 and 1, but limits of 0 and 255 were used to display maps. As a result, there was a 360x360 gray−scaled image. The gray level co−occurrence matrix of two perpendicular directions (0° and 90°) was computed and the following parameters were utilized (see Table 11 in section 2.2.4):

- uniformity of energy
- entropy
- homogeneity

These coefficients describe how homogeneous the image is. These chaotic maps have diagonal symmetry because of the absolute values in Eq.15. Example patterns are presented in Fig.15.

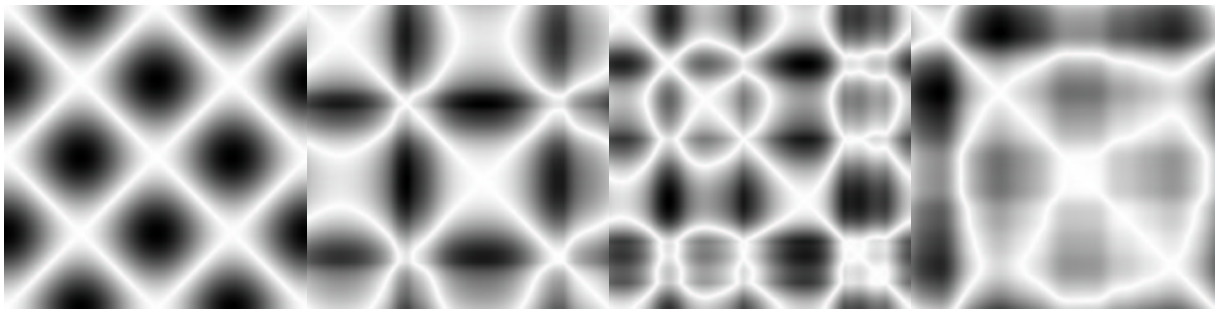

1.) 2.) 3.) 4.)

Fig.15: Chaotic map of 1 − sin(2x), 2 − wheat kernel,
3 − corn, 4 − string−pea

Rotation of the object has no effect on the statistical evaluation. If the data set is shifted, the map will be shifted along its diagonal (Fig.16).

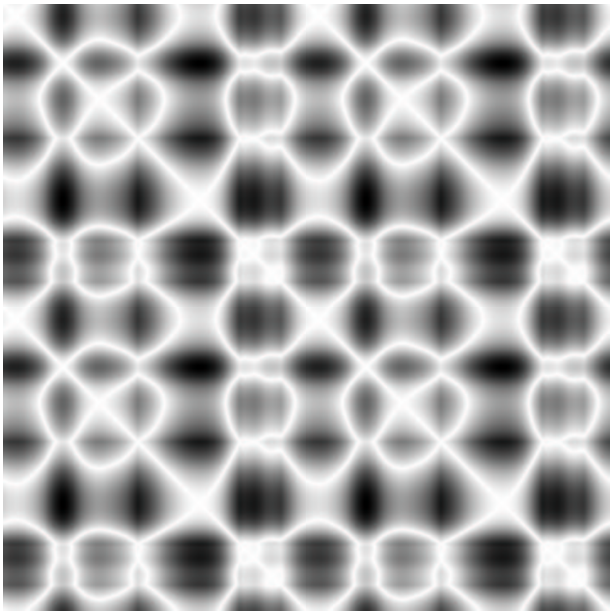

Fig.16: Tiled maps of a corn kernel

If the shape is similar to a plant fragment (see Fig.9/4 or Fig.14/4), the average radii of neighboring sectors may be considerably different and make a more complicated map. Figure 17 presents the map of the mentioned object.

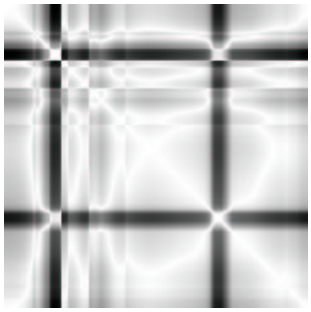

Fig.17: Effect of significant differences of neighboring radii

On the whole, there are six chaotic properties to evaluate regularity or irregularity of shapes: three attributes of the attractor and three texture parameters of the chaotic map.

4.5 Color measurement

The surface of the selected object was scanned and average intensities of red, green and blue color signals were calculated. To avoid effects of illumination on intensity, normalized values were used in the statistics:

$$r_n = \frac{255 \cdot \bar{R}}{\bar{R}+\bar{G}+\bar{B}} \qquad g_n = \frac{255 \cdot \bar{G}}{\bar{R}+\bar{G}+\bar{B}} \qquad b_n = \frac{255 \cdot \bar{B}}{\bar{R}+\bar{G}+\bar{B}} \qquad \text{(Eq.16)}$$

4.6 Evaluation of surface texture

All points of the object were compared to neighboring points and differences of intensity were collected into histograms (Fig.18). Four histograms were generated: one for gray level differences, and one for each color signal (red, green and blue). Texture analysis on gray−scaled images is a traditional technique to detect periodic patterns of the surface. They measure periodic changes of light parts and shade. This method was extended to color signals to describe color distribution.

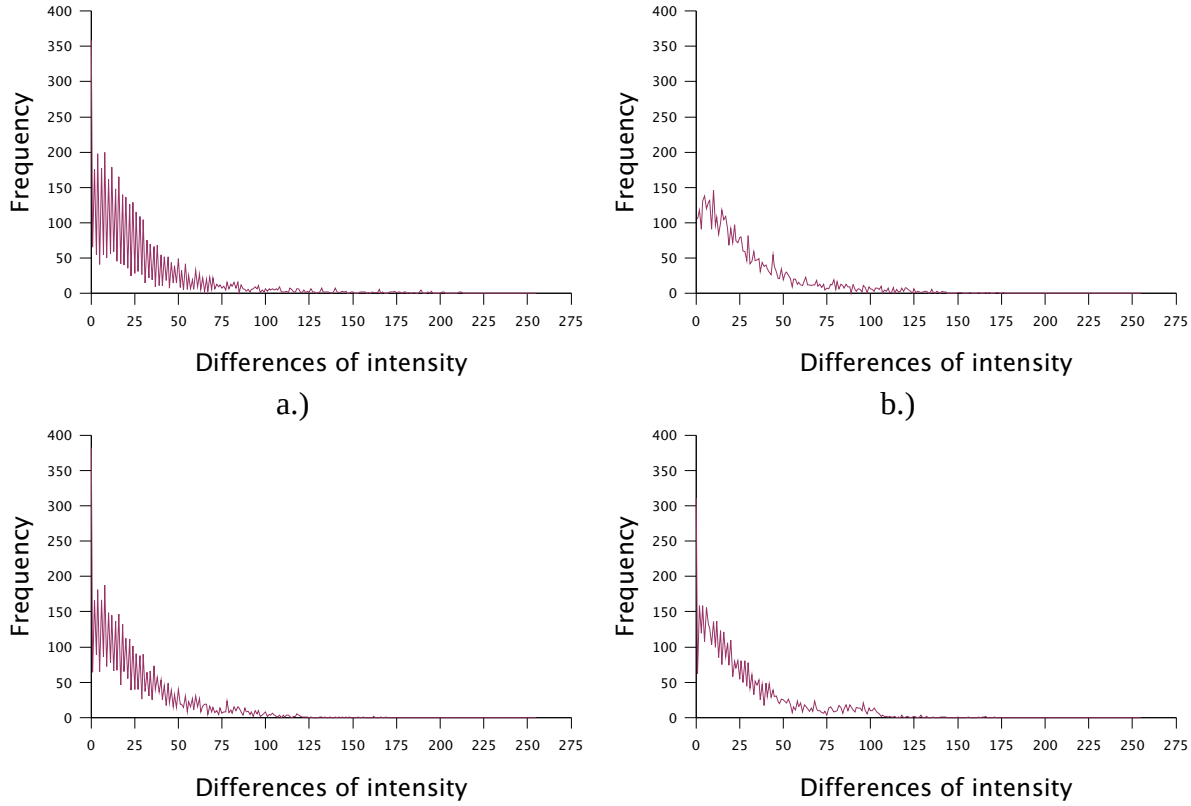

Fig.18: Histograms of differences in surface texture
a − blue, b − green, c − red, d − gray

These histograms show cumulative differences along two perpendicular directions (0° and 90°). First neighbors were compared with the following displacement vectors: $V_x[1;0]$ and $V_y[0;1]$.

Two concurrent approaches were tested in the qualification. The first one is called Polar Qualification System (Kaffka, Gyarmati, 1998). Figure 19 compares the gray histogram of a whole wheat kernel and a piece of foreign material. Projection of histograms into a two dimensional point causes considerable loss of information, but the position of the quality point shows dominant differences. It is unable to contribute to quantitative analysis, but it is able to discriminate histograms of distinct shapes.

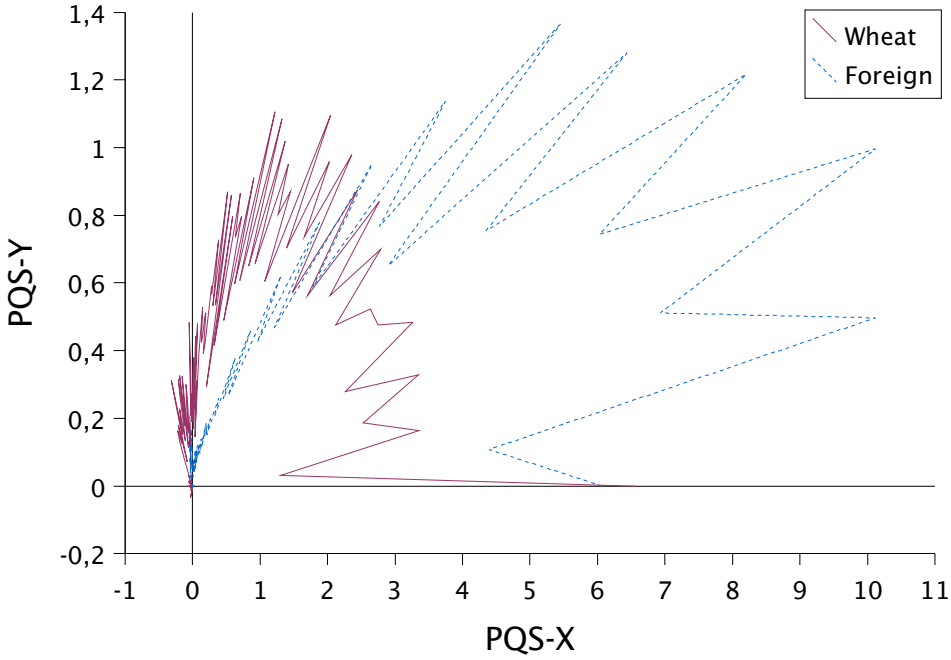

Fig.19: Curves of different textures in the polar diagram

In order to reduce the computation time necessary to calculate the co−occurrence matrix, first−order statistics can be computed on the image window (Jähne, Haußecker, Geißler, 1999b). This technique uses sum and difference histograms for gray levels. The following functions were used to evaluate the presented difference histograms:

Table 14: Histogram features

Parameter	Computation
Mean	$\mu = \sum i \cdot P(i)$
Angular Second Moment	$\sum \left(P(i)\right)^2$
Contrast	$\sum (i-\mu)^2 \cdot P(i)$
Entropy	$\sum -P(i) \cdot \log P(i)$

where *P(i)* gives the probability of a certain value scaled between 0 and 1 (number of pixels of intensity *i* is divided by the total number of pixels).

4.7. Statistical evaluation

4.7.1 Discriminant analysis

The basic concept of discriminant analysis is to maximize the distances between classes by transformation of variables. This method uses weighted linear combinations of quantitative variables to predict the discrete class to which an item belongs. The general form of the discriminant function is given by

$$L = b_1 x_1 + b_2 x_2 + \ldots + b_p x_p \qquad \text{(Eq.17)}$$

where L is a weighted linear composite score. The mean score for all cases combined is 0 and the pooled within−group variance is 1. The optimal set of coefficients (b_i) maximizes the ratio of between−group variability to the within−group variability of L. The greater the distances

are between the means, the better is the probability of success in classification. The maximum number of discriminant functions that can be derived is either one less than the number of groups or the number of discriminating variables, whichever is smaller. When the independent variables are not in standardized form, their coefficients are called unstandardized discriminant function coefficients. These may also be called canonical variates and unstandardized canonical discriminant functions. Statistical Program for Social Sciences (SPSS 8.0) and Statgraphics packages were used in the evaluation.

4.7.2 Distance function

Besides discriminant analysis, a normalized distance function was applied to evaluate the data sets. It compares attributes to the average and divides differences by the standard deviation (Eq.18).

$$D=\frac{x-\bar{x}}{SD} \qquad \text{(Eq.18)}$$

The advantage of this approach is that distance D is a dimensionless quantity and it is able to compare variables of different features with different scales. Owing to the normalization by the standard deviation, probabilities can be assigned to the results (provided that variables have normal distributions within a specific sub−group of the whole data set). Table 15 presents these limits for popular probability values.

Table 15: Assignment of D values

Probability	Deviation	D^2
68.23%	± SD	< 1
95.45%	± 2SD	< 4
99.73%	± 3SD	< 9

An example of the evaluation method based on these distances is presented in Table 16. A teaching sample set is selected to calculate means and standard deviations. Parameters of test object are compared with these values and the distances are computed. According to the limiting values for distance, the number of rejected attributes − parameters exceeding the limits − can be counted. If this number is higher than expectations, the object will not be classified into that group.

Table 16: Evaluation process with distance function

Teaching sample	Parameters						
	P1	P2	P3	P4	P5	P6	
Mean	7.75	0.38	0.78	172.0	19.74	32.49	
Deviation	0.06	0.01	0.2	44.6	3.42	2.33	
Test object	Parameters						
	P1	P2	P3	P4	P5	P6	
Measured	7.84	0.37	0.46	354.31	27.15	24.93	
Distance	1.5	−0.28	−1.58	4.08	2.16	−3.25	
Limit	Rejection						N
SD	+	−	+	+	+	+	5
2SD	−	−	−	+	+	+	3
3SD	−	−	−	+	−	+	2

5. Results and discussion

5.1 Outline estimation with sine functions

5.1.1 Sine function with variable period

A stepwise optimization algorithm − with least squares method − was applied to fit sine functions (Eq.11) to the outline. The goodness of estimation depends on the number of iterations, on the length of each step and on ε. Where ε is the tolerance limit for the differences between the sum of squares for successful iterations.

$$\varepsilon < SS_n - SS_{n+1} \qquad \text{(Eq.19)}$$

Variance analysis ranked possible values for ε. Table 17 presents the comparison of estimation of 200 whole wheat kernels in 9 different ε levels.

Table 17: Variance analysis for coefficients of determination

Source	SS	df	MS	Fisher	Sig. level
Model	1122192.3	8	140274.03	541.037	0.0000
Error	464350.8	1791	259.27		
Total	1586543.1	1799		Prob. level:	95.00 %

Analysis of variance proved that ε has an effect on the coefficient of determination (R^2). The probability of the null hypothesis is zero to four digits. On the other hand, Cochran's C test was 0.164638 (P=2.22875e−5), Bartlett's test was B = 1.58846 and P(827.274) = 0, and Hartley's test was 50.9255. These robust tests were used to confirm variance analysis, because common tests can fail in the case of other than normal distributions. Distances of classes were compared to the least significant differences, and the following similar groups were found (P=95%): ε values above 0.5, and ε values below 0.001. As expected, the R^2 values increased with decreasing values of ε (Fig.20).

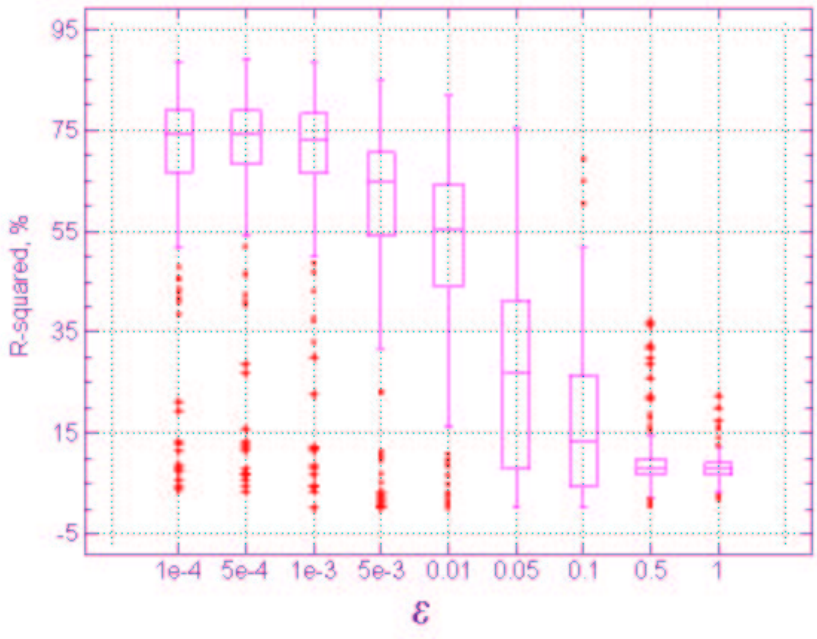

Fig.20: Changes of R^2 with decreasing value of ε

The presented diagram (Fig.20) confirmed the numeric results of analysis, and suggested 0.001 as the limiting value for ε. After a decision about this important parameter, coefficients of sine functions measured the following attributes:

- average radius
- vertical shift (mean value of the sine function compared to the average radius)
- amplitude
- period

The average radius was computed in the first step and radii values were normalized with it.

Discriminant analysis was used to classify whole wheat kernels, corn, broken wheat kernels and foreign objects (fragments of plants and insects). Table 18 presents the classification results based on the parameters of sine functions.

Table 18: Classification based on the parameters of sine functions

Predicted:	Broken	Corn	Foreign	Wheat	Pieces
Broken	100.00 %	0.00 %	0.00 %	0.00 %	56
Corn	0.00 %	99.03 %	0.97 %	0.00 %	310
Foreign	1.75 %	10.53 %	78.95 %	8.77 %	57
Wheat	9.95 %	0.00 %	0.00 %	90.05%	201

Three discriminant functions were supplied. Figure 21 presents the distribution of data points on the plane for the first two functions.

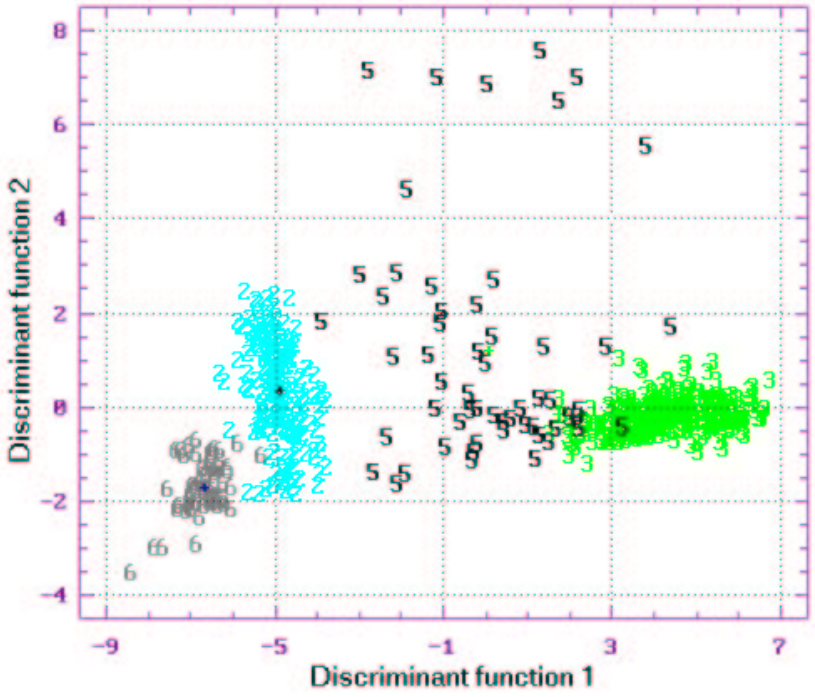

Fig.21: Classification results with sine functions of variable period
(codes are: 2 − wheat, 3 − corn, 5 − foreign, 6 − broken)

Pairwise discriminant analysis was performed to find optimal weights of parameters to discriminate between different classes of shapes. Results for pairwise classification are presented in Table 19.

Table 19: Pairwise classification with sine functions of variable period (% correct)

	Corn	Small	Broken	Foreign	Mix	Barley	Insect
Wheat	100	93.27	97.29	97.67	99.69	91.46	97.62
Corn		100	97.00	100	98.51	99.81	98.89
Small			98.83	98.05	77.84	97.07	95.62
Broken				97.35	83.94	97.74	95.37
Foreign					74.19	93.21	92.52
Mix						85.14	96.70
Barley							97.54

Pairwise comparison of whole wheat grains, small wheat grains and foreign materials with corn kernels provided 100% accuracy. Only four pairs out of the 28 had lower values (below 90%). Theoretically, an optimal decision tree can be built on the basis of Table 19. Figure 22 presents the result of discriminant analysis using the pairs of whole wheat and corn kernels (this is expected to be the first comparison of a binary decision tree).

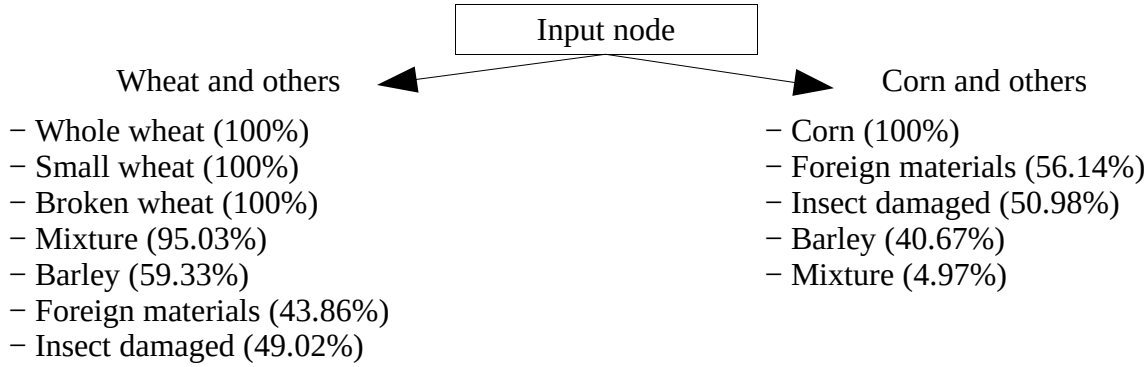

Fig.22: Division of samples into two basic types of shapes (corn and wheat types)

The effectiveness of classification of the groups presented in Figure 22 is lower than for Table 19, because the optimal discriminant functions for corn and wheat differ from the optimal discriminant function of other pairs. The whole decision tree is built from divisions similar to Figure 22.

Correlations between three classification parameters were high enough to suggest redundancy. There was a relationship between R^2 values and period with r = 0.86980, and between R^2 and amplitude of the sine function with r = 0.58309. All other correlations were further away from the limit, which is accepted to discriminate significant and random relationships. The distribution of points in Figure 23/a shows that the applied sine function was more accurate when the variance of radii was higher. The location of data points on Figure 23/b shows that the algorithm reached higher accuracy in modeling elliptical shapes, and the effectiveness in describing shape was very low in the case of asymmetric spherical shapes.

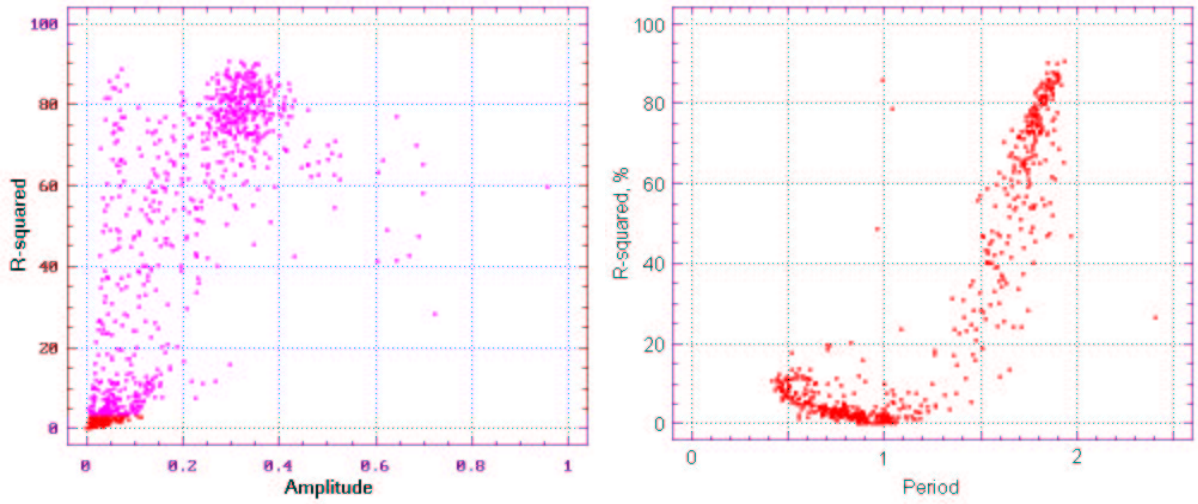

a.) b.)

Fig.23: Relationship between R^2 and amplitude (a), R^2 and period (b)

5.1.2 Sine functions with variable amplitudes

A more sophisticated function (Eq.12) was also applied. The benefit of this approach is that it revealed the asymmetry of shapes with elliptic bases (typical wheat kernels). The degree of deformation appeared in the amplitude of sin(x) and its position was also calculated as the differences of rotation of the fitted sin(x) and sin(2x) functions. In this case, the stepwise optimization algorithm required another ε (Eq.19). Table 20 presents the variance analysis of R^2 values, in relation to ε.

Table 20: Variance analysis for coefficients of determination

Source	SS	df	MS	Fisher	Sig. level
Model	781347.11	9	86816.345	1658.597	0.0000
Error	104163.03	1990	52.343		
Total	885510.14	1999		Prob. level:	95.00 %

According to these results, variances were significantly different for different values of ε. It was confirmed with robust tests: Cochran's C test: 0.27313 (P = 4.21885E−14), Bartlett's test: B = 1.77894, where P(1144.17) was zero again, and Hartley's test: 87.6707. Only one pair of ε values made a close group, where distance of centroids was lower than the least significant difference: values of 0.0001 and 0.00005 (1e−4 and 5e−5). These results and the following chart (Fig.24) recommend a lower value for ε, compared to the former estimation with variable periods.

Computation took 20 seconds with the sine functions of variable period and approximately 50 seconds with the sine functions of variable amplitudes (with a personal computer of Intel Celeron 300MHz processor, 128MB RAM, and Linux Mandrake 7.2 operating system). Unfortunately, the required time has no fixed value since it depends on the shape and initial optimization parameters.

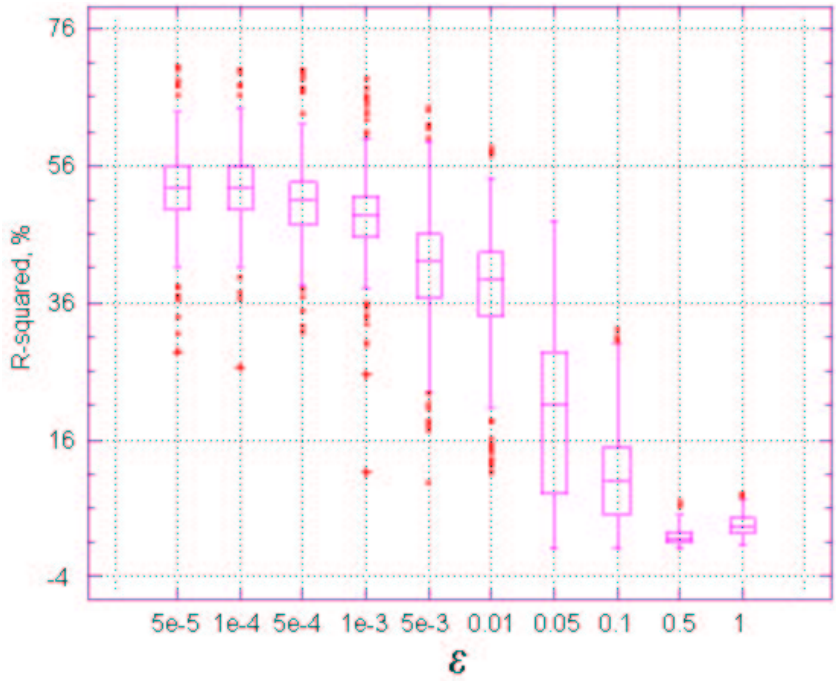

Fig.24: Changes of R^2 with decreasing value of ε

The average radius was computed first and all radii were normalized with it prior to calculating other parameters. As a result, there were five parameters to describe shape:

- average radius
- vertical shift (mean value of sine function compared to the average radius)
- amplitude
- degree of deformation
- position of deformation

Discriminant analysis was used to test the effectiveness of this algorithm. Table 21 presents the classification results with this sine function. Correct recognition of whole wheat kernels − and only this one − was higher compared to the former results with sine functions of variable periods. The highest correlation (r=0.49268) occurred between vertical shift and position of deformation. No parameters were highly correlated as to be redundant.

Table 21: Classification accuracy based on parameters of sine functions

Predicted:	Broken	Corn	Foreign	Wheat	Pieces
Broken	96.43 %	0.00 %	0.00 %	3.57 %	56
Corn	0.00 %	97.42 %	2.58 %	0.00 %	310
Foreign	0.00 %	12.28 %	75.44 %	12.28 %	57
Wheat	2.49 %	0.00 %	0.00 %	97.51 %	201

Figure 25 presents the projection of data points on the plane of the first and second discriminant functions. Figure 21 and Figure 25 are similar. The group of foreign materials is located between the clusters of whole wheat and corn kernels. According to the values in Table 18 and Table 21, both sine functions are able to estimate elliptical, triangular and asymmetric shapes. The shape of whole wheat kernels is basically elliptical with some asymmetry. This is why the sine functions of variable amplitudes could improve the recognition rate. This special shape does not apply to the others, as reflected by poorer classification for other groups.

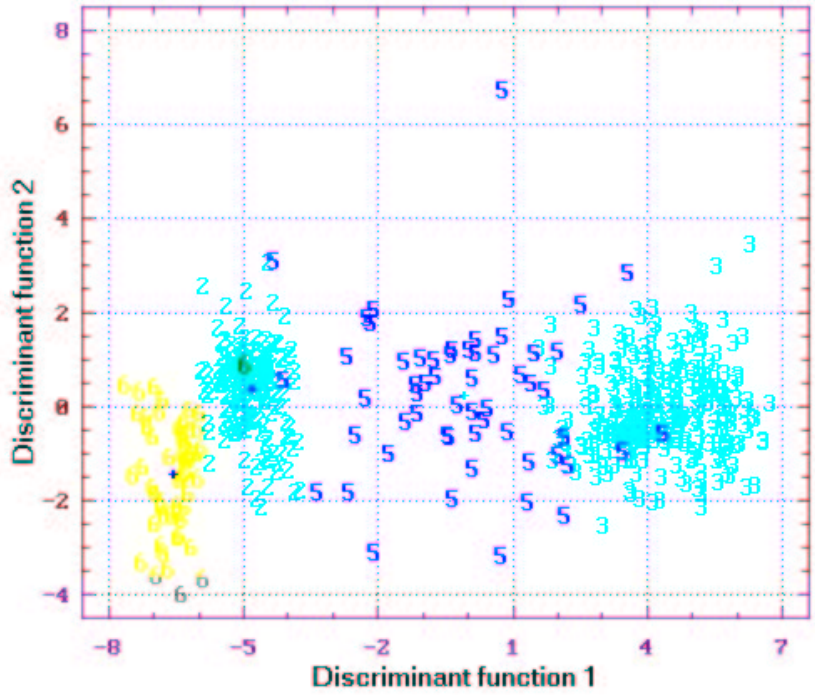

Fig.25: Classification results with sine functions of variable amplitudes
(codes are: 2 − wheat, 3 − corn, 5 − foreign, 6 − broken)

The results of pairwise classification by discriminant analysis are presented in Table 22. The first node (Fig.26) of the decision tree (based on the values of Table 22) is similar to the first node of the previous decision tree (Fig.22) of sine functions of variable period. Classification of barley is improved, with the accuracy reaching 100% in the first step (compared to 59.33% in Fig.22).

Table 22: Pairwise classification with sine functions of variable amplitudes (% correct)

	Corn	Small	Broken	Foreign	Mix	Barley	Insect
Wheat	100	93.27	97.29	97.67	68.51	91.22	97.62
Corn		100	97.00	100	98.73	99.81	98.89
Small			98.83	97.66	79.22	96.33	96.41
Broken				97.35	83.49	97.37	94.44
Foreign					73.73	92.83	93.46
Mix						89.73	97.17
Barley							91.54

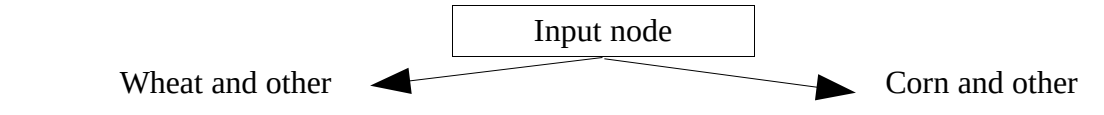

− Whole wheat (100%)
− Small wheat (100%)
− Broken wheat (100%)
− Barley (100%)
− Insect damaged (98.04%)
− Mixture (95.03%)
− Foreign (45.61%)

− Corn (100%)
− Foreign (54.93%)
− Mixture (4.97%)
− Insect damaged (1.96%)

Fig.26: First node of decision tree with parameters of sine functions of variable amplitudes

5.2 Polynomial regression on outline

As a result of polynomial regression, the following parameters were used in classification: average radius, coefficient of determination (R^2), coordinates of quality point and area of smallest covering rectangle of the polynomial coefficients plotted with polar coordinates (Fig.12 in section 4.4.2). Table 23 presents the effectiveness of classification of broken and whole wheat grains, corn kernels and foreign materials.

Table 23: Classification based on polynomial coefficients

Predicted:	Broken	Corn	Foreign	Wheat	Pieces
Broken	91.07 %	0.00 %	0.00 %	8.93 %	56
Corn	0.00 %	97.42 %	2.58 %	0.00 %	310
Foreign	0.00 %	12.28 %	77.19 %	10.53 %	57
Wheat	3.48 %	0.00 %	0.00 %	96.52 %	201

The distribution of data points on the plane of the first two discriminant function is presented in Figure 27.

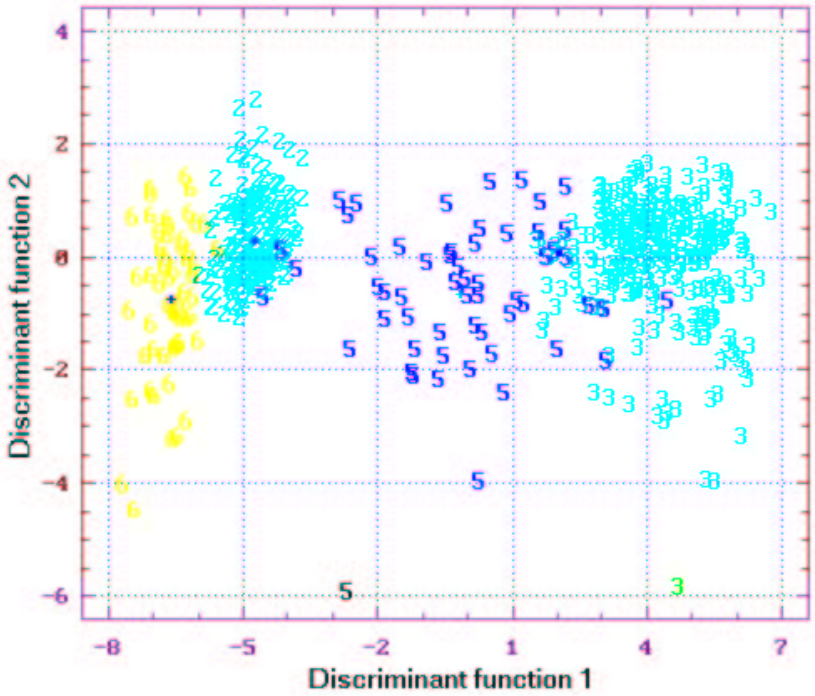

Fig.27: Classification results with polynomial regression
(codes are: 2 − wheat, 3 − corn, 5 − foreign, 6 − broken)

Pairwise discriminant analysis was done to find the best classification functions between the groups of tested materials. The result of pairwise classification is presented in Table 24. Although values of Table 24 and Table 22 are different, the first node of their decision trees are identical.

Table 24: Pairwise classification with parameters of polynomial regression (% correct)

	Corn	Small	Broken	Foreign	Mix	Barley	Insect
Wheat	100	91.77	97.67	97.67	64.92	97.07	61.51
Corn		100	95.10	100	97.24	100	99.72
Small			98.05	83.20	56.51	99.76	73.71
Broken				97.35	81.19	95.86	91.67
Foreign					66.82	99.62	85.05
Mix						85.68	53.30
Barley							95.00

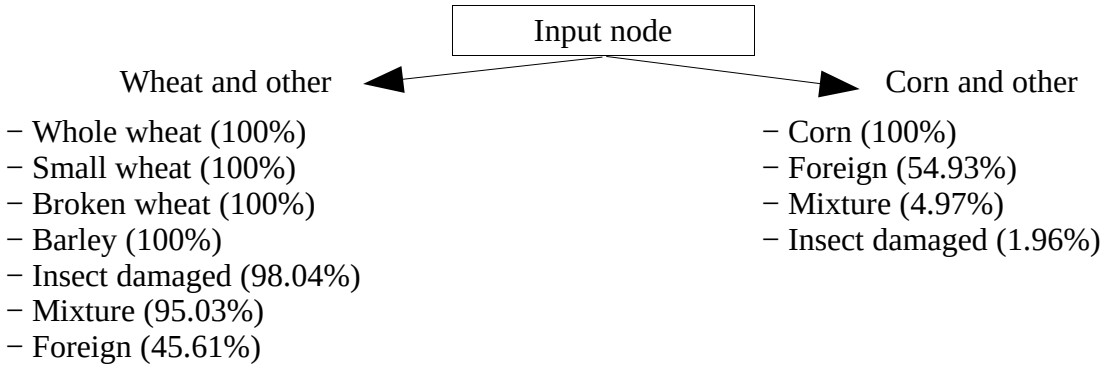

Fig.28: First node of decision tree with polynomial regression

There was close correlation between coordinates of the quality point (PQS_x and PQS_y) with r=0.9776 and they correlated with area of smallest covering rectangle (r=0.8398). A quadratic relationship was found between PQS_y and area attributes. Table 25 presents the analysis of variances for the quadratic regression.

Table 25: Variance analysis for regression

Source	SS	df	MS	Fisher	Sig. level
Model	1.7360e16	3	5.7968e15	9.9999e4	0.0000
Error	7.6647e12	981	7.8052e9		
Total	1.7368e16	984		Prob. level:	95.00 %

Equation for regression (parabola):

$$Y = a \cdot (X - u)^2 + v \qquad \text{(Eq.20)}$$

where *a* is a multiplicative factor, and minimum point of parabola is located at P(*u*;*v*). Figure 29 shows data points with the fitted curve and the distribution of residuals.

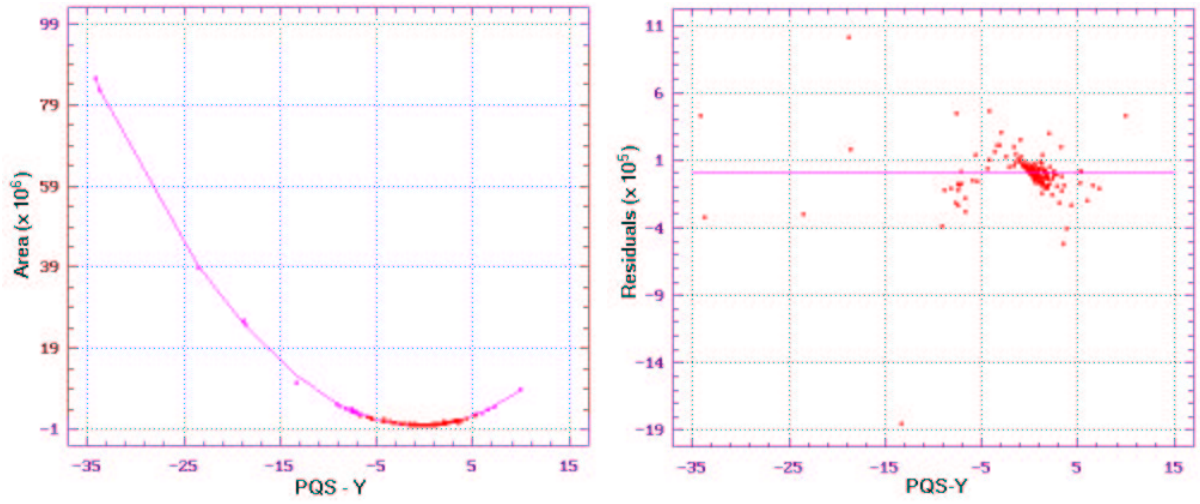

a.) b.)

Fig.29: Fitted parabola (a) and distribution of residuals (b)

There is no trend in residuals (Fig.29/b). This was confirmed with Durbin−Watson statistics (D=1.97967). Discriminant function coefficients for parameter "Area" are zero for five digits (Table 26).

Table 26: Unstandardized discriminant function coefficients

Parameter	1	2	3
Average radius	0.18721	0.00564	0.00698
PQS_x	0.00221	0.15102	0.43973
PQS_y	−0.02384	0.42885	1.15959
R^2	0.00985	0.08963	−0.03752
Area	0.00000	0.00000	0.00000
Constant	−11.6198	−7.39904	2.08551

According to the close quadratic relationship and low values in Table 26, parameter "Area" can be ignored (it seems to contain redundant information).

5.3 Chaotic parameters of shape

Two different approaches were used to measure chaos in shape. The attractor was evaluated with three parameters: area of smallest covering rectangle, area occupied by points of the attractor within this rectangle, perimeter index. The difference matrix was computed and chaotic maps were evaluated with another three parameters: uniformity of energy, entropy and homogeneity. The classification results with chaotic parameters are shown in Table 27.

Table 27: Classification based on chaotic properties

Predicted:	Broken	Corn	Foreign	Wheat	Pieces
Broken	98.21 %	0.00 %	0.00 %	1.79 %	56
Corn	0.00 %	99.68 %	0.32 %	0.00 %	310
Foreign	0.00 %	22.81 %	77.19 %	0.00 %	57
Wheat	0.50 %	0.00 %	0.00 %	99.50 %	201

This method utilizes only symmetry information and the complexity of the outline. The results of pairwise classification with chaotic properties of grains are presented in Table 28.

Table 28: Pairwise classification with chaotic parameters (% correct)

	Corn	Small	Broken	Foreign	Mix	Barley	Insect
Wheat	100	84.04	93.41	98.05	95.30	98.54	80.16
Corn		99.22	89.10	90.71	84.71	99.81	89.75
Small			91.44	97.66	92.52	99.76	76.10
Broken				78.76	61.01	92.48	72.22
Foreign					75.12	99.25	85.98
Mix						92.7	76.89
Barley							93.08

The first node of the decision tree based on chaotic parameters is presented in Figure 30.

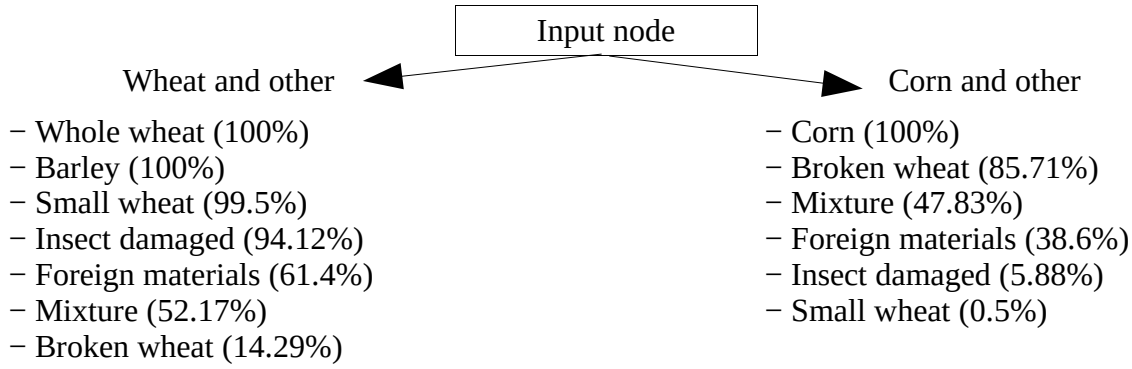

Fig.30: First node of decision tree with chaotic properties of shape

A high correlation was observed between the parameters for chaotic maps (Fig.31). This close relationship did not decrease the effectiveness of these parameters for classification.

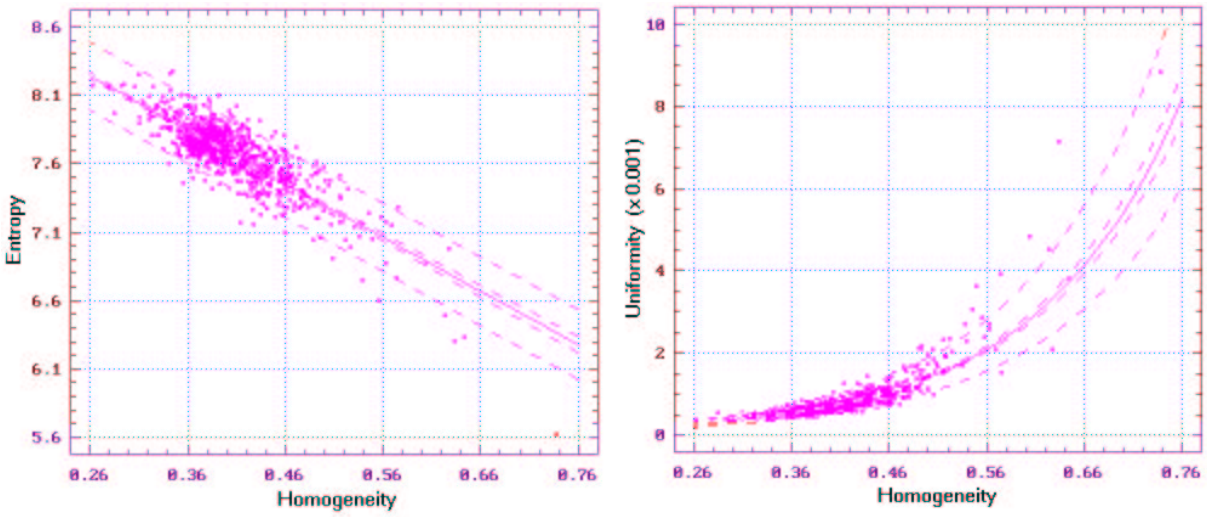

a.) b.)

Fig.31: Relationships between entropy, uniformity and homogeneity variables

Although the linear correlation between the relative area of attractor and the perimeter index was low (r=0.17567), a reciprocal function fitted their data pairs quite closely (Table 29).

Table 29: Variance analysis for regression

Source	SS	df	MS	Fisher	Sig. level
Model	142468.38	1	142468.36	3086.7	0.0000
Error	45370.794	983	46.155		
Total	187839.17	984		Prob. level:	95.00 %

According to this analysis, the relative area is redundant and should be excluded or the computation of perimeter index should be changed.

There are two ways to draw trajectories of attractors. One of them is to walk along the whole outline by given angles (Fig.32/c). The second − and better one − is to walk along the total outline by pixels (Fig.32/d). Although they are similar, the second approach was able to discriminate different shapes with higher accuracy.

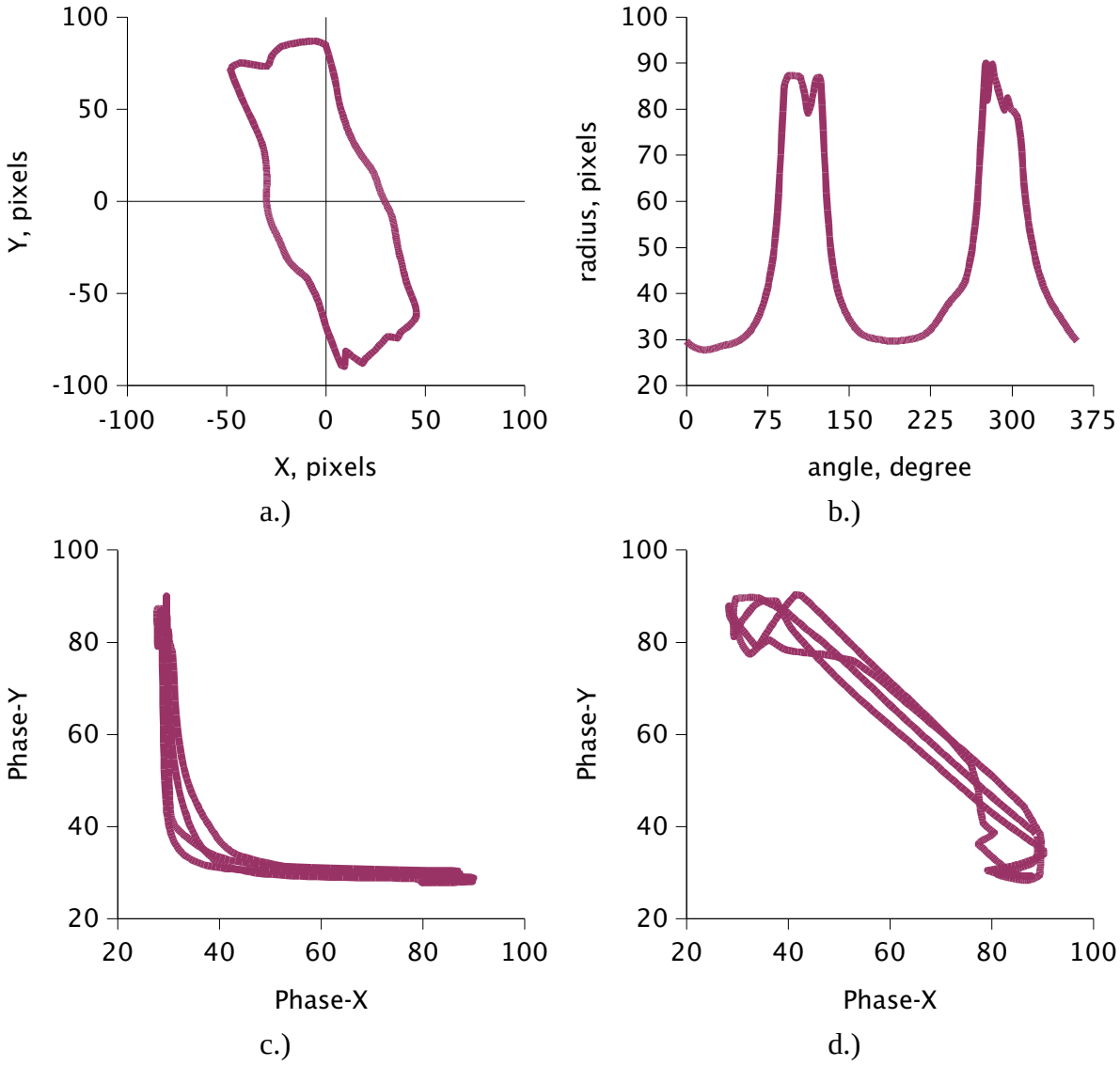

Fig.32: Original shape of a fragment of a stem and its attractors
(a − XY outline, b − polar outline, c − attractor by angles, d − attractor by pixels)

5.4 Color information

Color information is very important in human perception, and it must be included in the set of parameters. Normalized red, green and blue intensity values were computed (Eq.16) on the whole surface of objects. Because of the wide range of colors of grains and other objects in the samples, all color attributes (red, green and blue) were utilized. This decision was confirmed with principal component analysis. The following figure (Fig.33) shows how unit vectors of the original space were projected onto the plane of greatest separation.

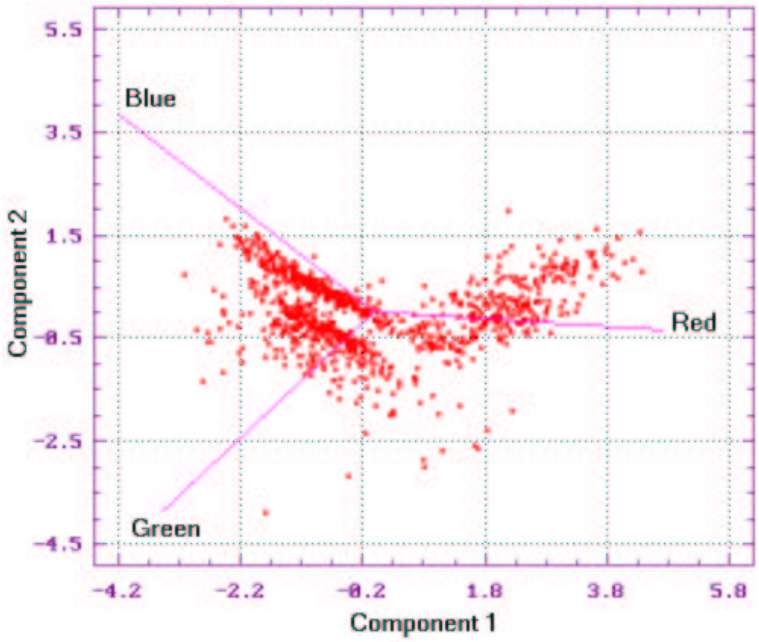

Fig.33: Color vectors and data points on the plane of maximal variance

The color vectors divided the selected plane into three parts. The directions of these color vectors help to distinguish classes of data points. Classification results based on discriminant analysis are shown in Table 30.

Table 30: Classification based on color information

Predicted:	Broken	Corn	Foreign	Wheat	Pieces
Broken	61.82 %	0.00 %	25.45 %	12.73 %	56
Corn	0.00 %	96.75 %	0.00 %	3.25 %	310
Foreign	50.00 %	0.00 %	29.63 %	20.37 %	57
Wheat	1.56 %	0.00 %	25.45 %	80.21 %	201

Basic statistics for color values are presented in Table 31.

Table 31: Statistics of normalized color values

Mean	Wheat	Corn	Foreign	Broken
Red	102.097	119.593	96.0567	96.0235
Green	87.2640	80.8897	88.0706	87.1243
Blue	65.6390	54.5170	70.8727	71.8522
Std.dev.	**Wheat**	**Corn**	**Foreign**	**Broken**
Red	2.95719	5.78900	3.59768	2.66937
Green	0.45366	4.20874	1.15617	0.50578
Blue	2.76826	2.70527	3.92001	2.88193

Because of the dominant red color, corn kernels were recognized with the highest success rate (96.75%). Because of the similar color of broken wheat kernels and the foreign materials tested, 50% of foreign materials were classified as broken wheat and 25.45% of broken wheat grains were assigned to the foreign materials class.

5.5 Texture analysis

5.5.1 Evaluation based on PQS method

The surfaces of selected objects were scanned in perpendicular directions and the differences of intensity were collected into histograms. Two displacement vectors selected pixels for comparison: $V_y(0;dy)$ and $V_x(dx;0)$. Values of *dx* and *dy* define the distance between points of interest (length of displacement vector). In order to avoid dependence on rotation of the surface pattern, *dx* and *dy* must be equal. The effects of length of these vectors were tested up to 20% of the average radius of whole wheat kernels. Figure 34 presents, how discriminant analysis was able to distinguish texture parameters computed with different length of vectors.

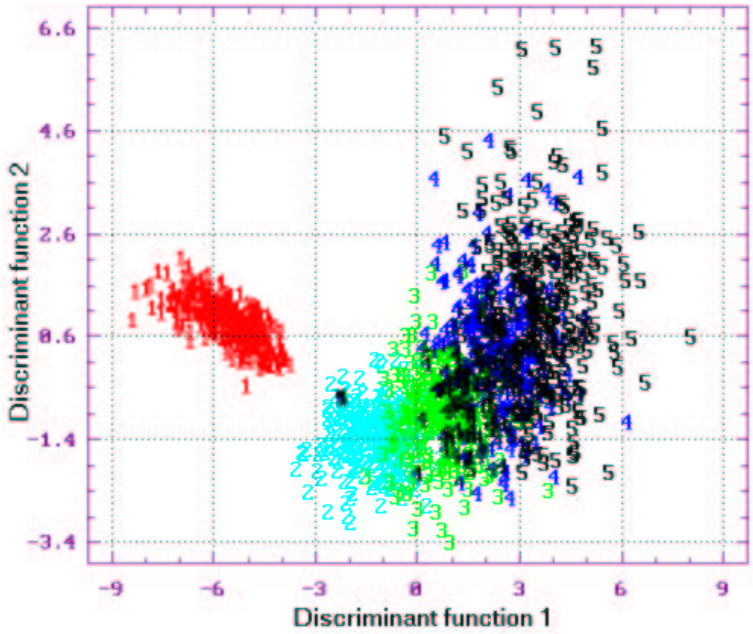

Fig.34: Affect of length of displacement vector on data points
(codes identify length in pixels)

According to this analysis, the lengths of vectors V_x and V_y have significant effects on the data. The deviation within classes increased with increasing length. This deviation affects the effectiveness of classification because of the increasing overlap. As a result, $dx = dy = 1$ distances were chosen. Table 32 presents the results of classification using only the gray level differences.

Table 32: Classification based on PQS coordinates of gray level differences

Predicted:	Broken	Corn	Foreign	Wheat	Pieces
Broken	98.18 %	0.00 %	0.00 %	1.82 %	56
Corn	0.00 %	94.77 %	5.23 %	0.00 %	310
Foreign	0.00 %	11.11 %	72.22 %	16.67 %	57
Wheat	2.60 %	0.00 %	0.00 %	97.40 %	201

Gray level differences indicate the periodic patterns of shade and light on the surface, and are able to describe its three−dimensional complexity. The color distributions and the regular pattern of color signals were represented by histograms of differences in color. Red, green, blue and gray quality points created eight parameters (PQS_x and PQS_y for each signal). The classification results with these attributes are shown in Table 33.

Table 33: Classification with PQS coordinates of color signals and intensity

Predicted:	Broken	Corn	Foreign	Wheat	Pieces
Broken	100.00 %	0.00 %	0.00 %	0.00 %	56
Corn	0.00 %	100.00 %	0.00 %	0.00 %	310
Foreign	7.41 %	1.85 %	90.74 %	0.00 %	57
Wheat	0.00 %	0.00 %	0.00 %	100.00 %	201

The previous two tables (Tables 32 and 33) contain results for the original histograms without normalization. This is the reason why it was able to distinguish broken and whole wheat grains. Normalization eliminates the effect of the size of the visible surface area. In the case of repeated tests with normalized values, the classes became too close to distinguish and separate successfully. Success rates were between 40% and 60%. Figure 35 shows the distribution of data points (without normalization) on the plane of the greatest separation.

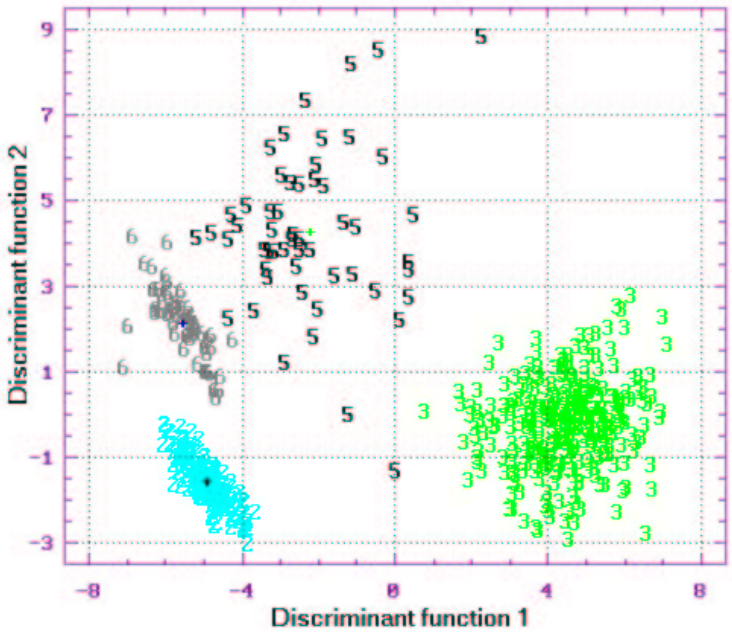

Fig.35: Distribution of PQS data sets
(codes are: 2 − wheat, 3 − corn, 5 − foreign, 6 − broken)

Table 34: Pairwise classification with all texture parameters (% correct)

	Corn	Small	Broken	Foreign	Mix	Barley	Insect
Wheat	100	99.48	97.15	100	88.67	98.49	99.16
Corn		100	98.61	100	99.57	100	100
Small			97.60	90.44	71.43	99.75	76.35
Broken				94.50	89.30	96.14	92.93
Foreign					68.06	100	87.00
Mix						87.70	45.63
Barley							99.60

Table 34 presents the results of pairwise classification with discriminant analysis of PQS coordinates for color signals and intensity. The first node of the decision tree with texture parameters is presented in Figure 36.

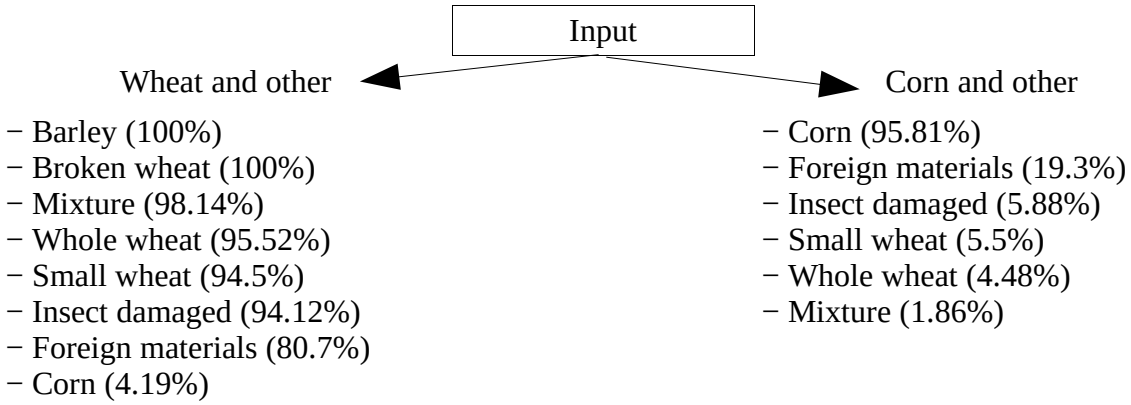

Fig.36: First node of decision tree with parameters of surface texture

5.5.2 Evaluation with other methods

Unser has suggested the computation of mean, angular second moment, contrast and entropy of difference histograms (see Table 14 in section 4.6). Because this computation is based on probabilities, the effect of the size of the visible area is automatically eliminated.

Table 35: Classification based on Unser's method

Predicted:	Broken	Corn	Foreign	Wheat	Pieces
Broken	10.91 %	0.00 %	0.00 %	89.09 %	56
Corn	0.00 %	46.08 %	53.92 %	0.00 %	310
Foreign	0.00 %	38.89 %	46.30 %	14.81 %	57
Wheat	0.52 %	0.00 %	0.00 %	99.48 %	201

Many broken grains were put into the whole wheat class, only if the shape of the object was changed (Table 35). In the cases of visible endosperm, broken grains were identified properly.

Another alternative method was based on the first ten values of the difference histograms. Figure 18 presented (see section 4.6) color and gray level histograms. There are high values near zero difference and lower ones with increasing differences. This is the reason why quality points are in the first quadrant (see Fig.19) and the size of the object has a significant effect. The first ten elements of the frequency data sets contain most of the available information. This was proven by statistical analysis as shown by the result in Table 36.

Table 36: Classification based on the first ten items of histograms

Predicted:	Broken	Corn	Foreign	Wheat	Pieces
Broken	100.00 %	0.00 %	0.00 %	0.00 %	56
Corn	0.00 %	99.02 %	0.98 %	0.00 %	310
Foreign	9.26 %	5.56 %	85.19 %	0.00 %	57
Wheat	0.00 %	0.00 %	0.00 %	100.00 %	201

Classification based on Unser's parameters (Table 35) and frequencies (Table 36) achieved lower accuracy than the PQS method (Table 33).

5.6 Optimal parameter set

There are basically three different types of visual information: shape, color and texture. They are used in human decisions when experts inspect samples. There is a need for one parameter set, so that computers can model the sophisticated human decision−making process. According to the introduced results, the following set was the best:

- Shape description:
  a.) polynomial regression
  − average radius
  − quality point of polynomial coefficients: PQS_x and PQS_y
  − coefficient of determination: R^2
  b.) chaotic parameters of attractor
  − relative area
  − covered area of graph on the phase plane
  − perimeter index
  c.) symmetry parameters of difference map
  − uniformity of energy
  − entropy
  − homogeneity
- Color measurement: normalized color vector
  − red intensity
  − green intensity
  − blue intensity
- Texture analysis: quality points of color and gray level difference histograms
  − quality point for red signal: PQS_x and PQS_y
  − quality point for green signal: PQS_x and PQS_y
  − quality point for blue signal: PQS_x and PQS_y
  − quality point for gray levels: PQS_x and PQS_y

On the whole, there are 21 parameters: 10 for shape, 3 for color and 8 for texture. The number of parameters belonging to each feature balances the importance of the features. There are 6 chaotic or symmetry attributes out of the 10 shape parameters, which is reasonably assuming that regularity has special dominance in human decisions.
Discriminant analysis successfully distinguished four classes of objects: broken wheat kernels, corn kernels, foreign materials (stones, fragments of plants, fragments of insects) and whole wheat kernels (Table 37).

Table 37: Classification with discriminant analysis based on 21 parameters

Predicted:	Broken	Corn	Foreign	Wheat	Pieces
Broken	98.18 %	0.00 %	0.00 %	1.82 %	56
Corn	0.00 %	100.00 %	0.00 %	0.00 %	310
Foreign	0.00 %	1.85 %	98.15 %	0.00 %	57
Wheat	0.00 %	0.00 %	0.00 %	100.00 %	201

Only two objects out of the 624 were misclassified. Figure 37 presents classification of ungrouped cases (small wheat kernels and a mixture of foreign materials like string pea and weed seeds).

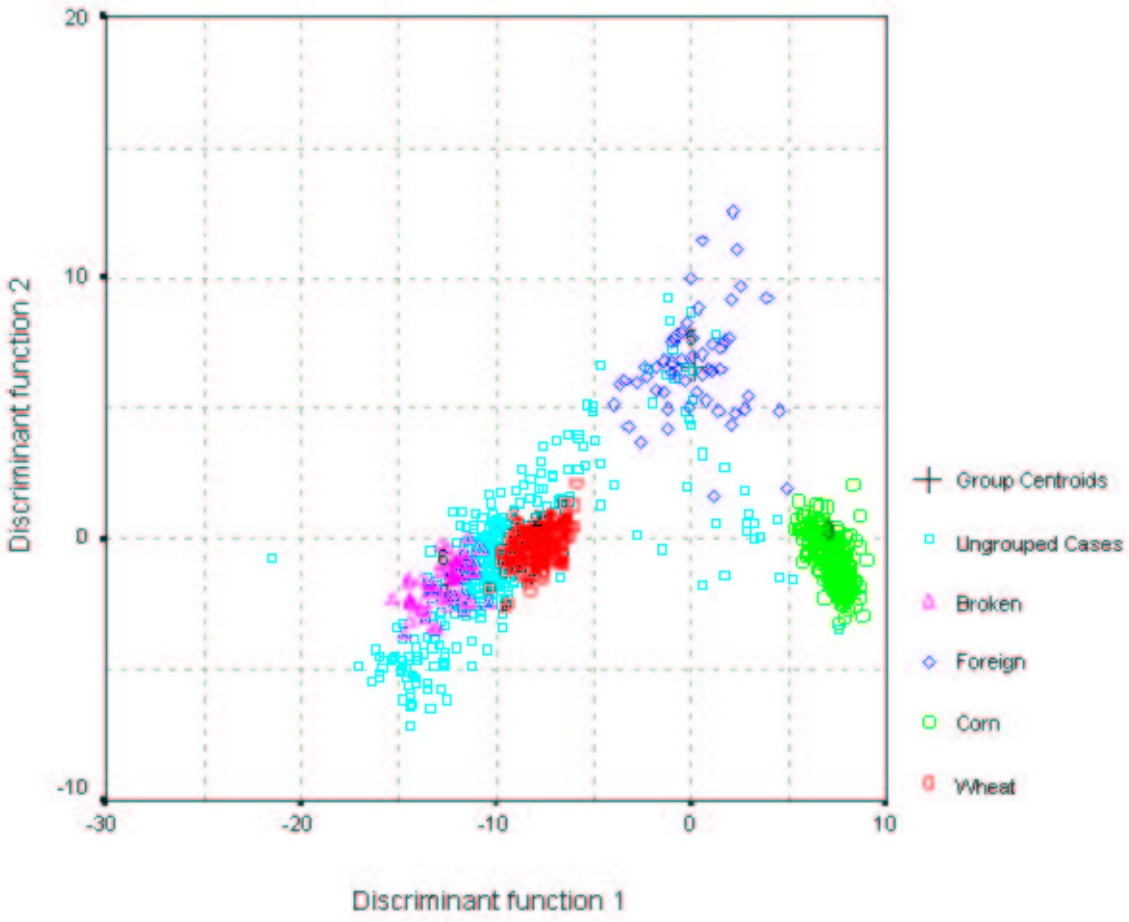

Fig.37: Distribution of data points on the plane of discriminant functions

Points for ungrouped cases (mixture, see Table 12) are located mainly between the broken and whole wheat classes. Small wheat kernels were expected to be near the whole ones, but this does not apply to other non−wheat objects in the sample. Of course, including them in the teaching set for discriminant analysis increased their correct recognition. Pairwise discriminant analysis was performed with an optimal parameter set (Table 38).

Table 38: Pairwise classification with optimal parameter set (% correct)

	Corn	Small	Broken	Foreign	Mixture	Barley	Insect
Wheat	100	100	100	99.60	99.15	100	99.14
Corn		100	99.72	100	99.79	100	100
Small			99.60	100	93.84	100	98.73
Broken				100	96.74	98.46	96.81
Foreign					88.79	99.62	94.74
Mixture						99.18	94.53
Barley							99.18

This table has only one value lower than 90%, in the case of pairs of mixture and foreign materials. The optimal decision tree for this parameter set and its effectiveness of classification are presented in Figure 38.

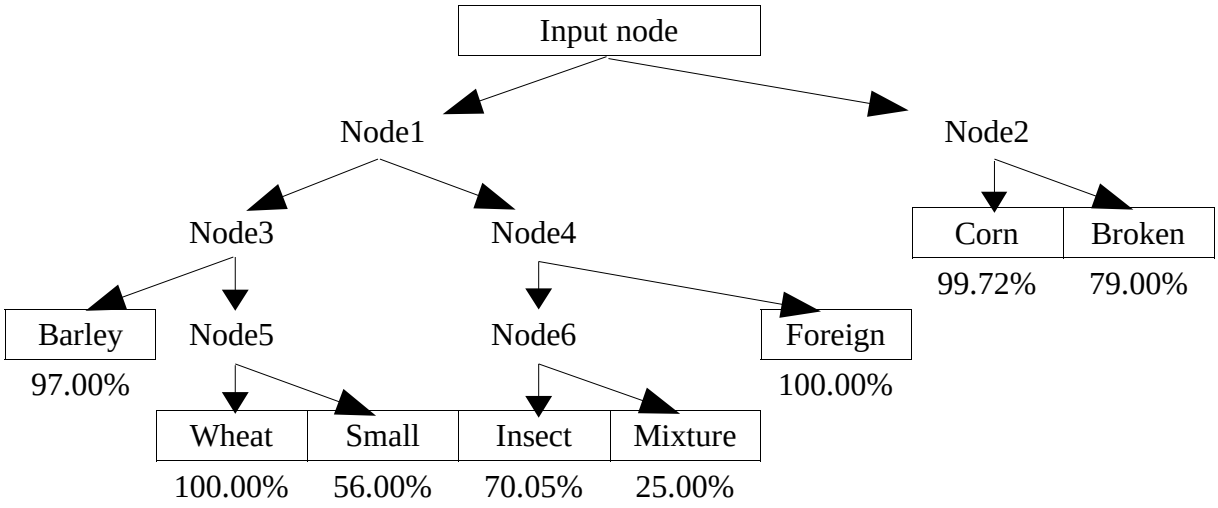

Where:

- Node1: wheat and other materials
- Node2: corn and broken wheat grains
- Node3: wheat and barley
- Node4: all foreign materials
- Node5: large and small wheat grains
- Node6: insect damaged kernels and mixture

Fig.38: Decision tree with optimal parameter set

Valuable grains (wheat, barley) are separated from foreign materials at Node1. At Node1, only 56.12% of small wheat grains and 56.52% of the mixture follow the correct pathway. In addition, only 57.14% of mixture was classified correctly at Node4. This is the reason why the mixture sample obtained low classification effectiveness. Large wheat grains and foreign materials (materials passing through the first sieve for wheat) were identified with 100% accuracy.

There is yet another method to classify objects. It is based on simple statistics for parameters (see Eq.18). The 21−dimensional Mahalanobis distance − normalized with standard deviation − for 21 parameters is able to separate classes with high accuracy. Figure 39 shows distances measured from the center of the group for whole wheat kernels.

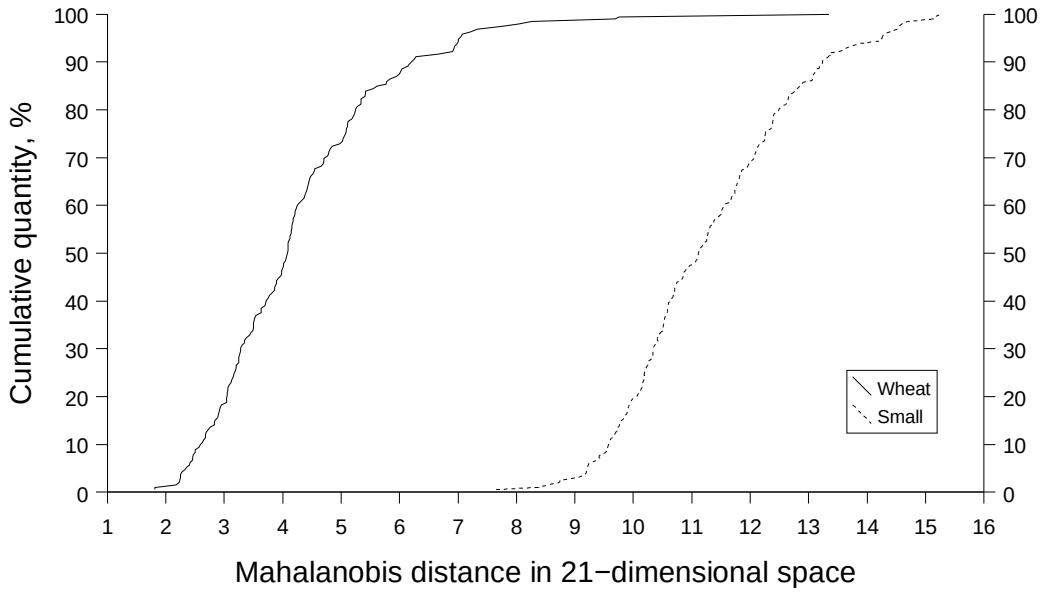

Fig.39/a.) Whole and small wheat grains

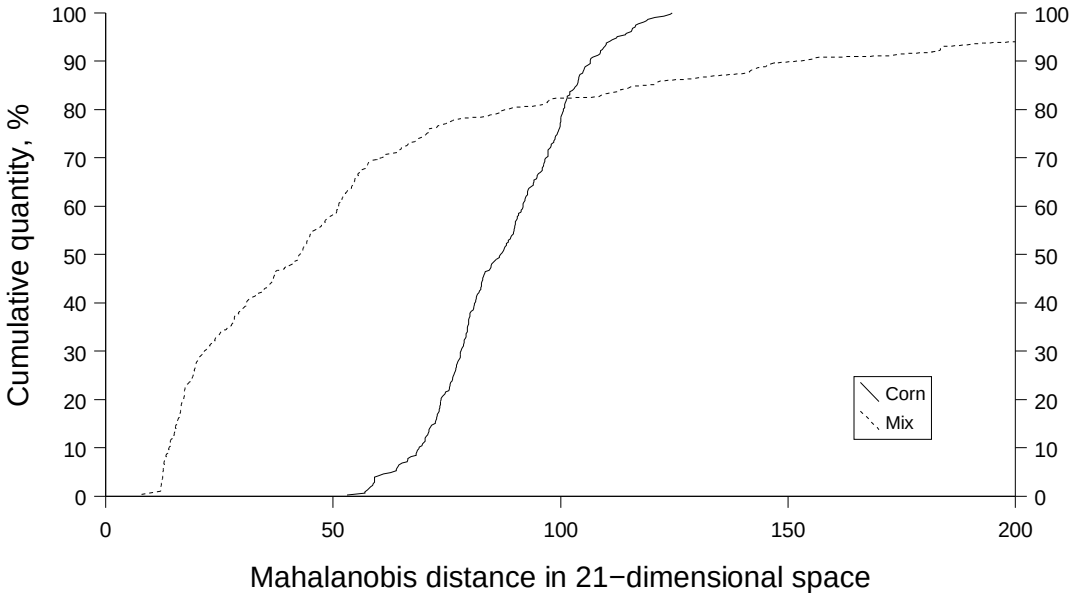

b.) Corn kernels and mixture of foreign materials

Fig.39: Distances measured from the center for whole wheat grains

Because the distance is measured in standard deviations, values along the X axis mean probabilities as well. If one limiting value for distance is selected, these diagrams will show the quantity of accepted and rejected objects in the group of whole wheat. For example, if this value is set to 8, 97.92% of whole and 0.51% of small wheat grains will be accepted (Fig.39/a). This overall distance function can fail if the parameter set contains variables with high correlations. The distribution of data points follows a certain direction in that case which direction depends on the variables and their correlations.

In order to increase the flexibility of classification, analysis of individual parameters has to be done. A simple distance function (Eq.18) is able to compare only one parameter to the average of the teaching sample. There are two options in this method:
– limiting value for distance function (D_{lim})
– limiting value for parameter values exceeding the selected limit (N_{lim})
Table 39 presents how the effectiveness of classification depends on these variables. The same trend was observed in the case of corn and barley kernels. As a result, a limiting value of 3 was selected for both variables.

Table 39: Discrimination of wheat and non−wheat objects (% correct)

	N_{lim}				
D_{lim}	1	2	3	4	5
1	84.18%	85.01%	86.66%	90.61%	89.95%
2	97.36%	97.53%	98.02%	91.93%	91.60%
3	99.18%	99.18%	99.51%	90.94%	90.94%
4	96.38%	96.38%	96.05%	90.61%	90.61%
5	92.26%	92.09%	91.93%	90.61%	90.61%

The following figure (Fig.40) compares how many times individual parameters exceeded this distance function limit.

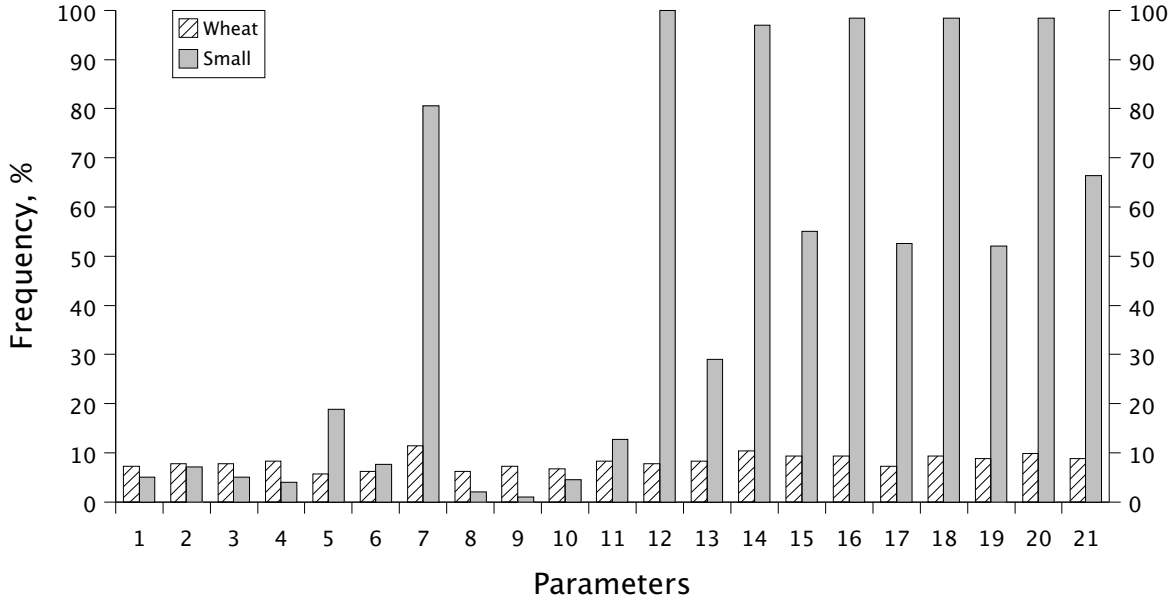

a.) Whole and small wheat kernels

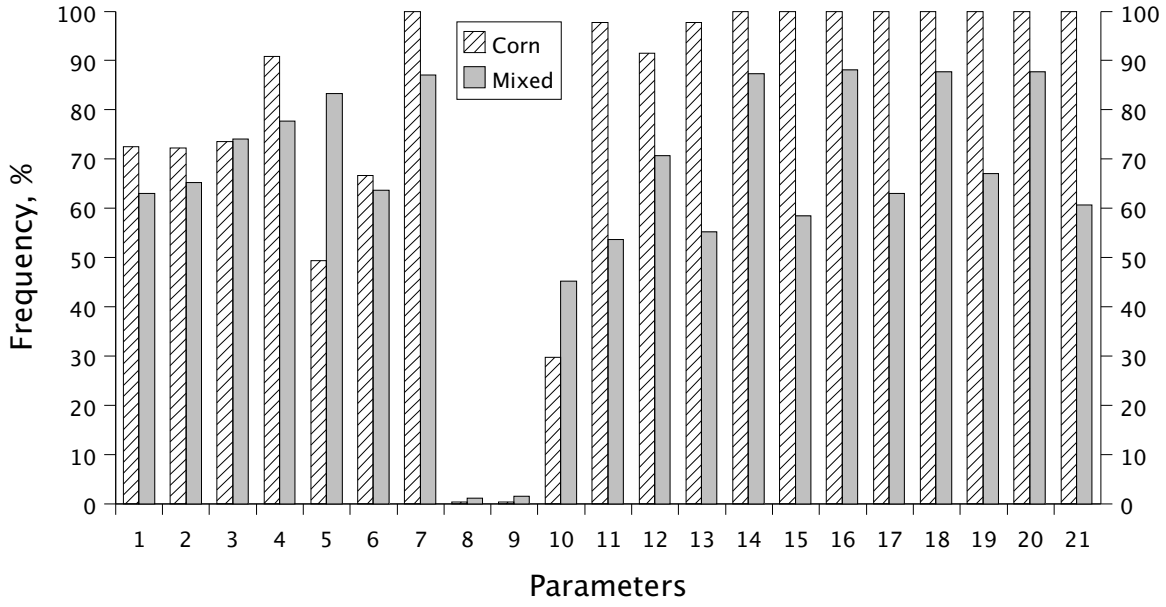

b.) Corn kernels and mixture of foreign materials

Fig.40: Frequency of rejection of parameters
(in group of whole wheat, limiting value is 3)

Frequency values were under 11.5% for whole wheat grains. According to Figure 34/a, small and whole wheat kernels differ in texture (#14−#21) and average radius (#7). They also differ in green color signal (normalized color values were used: #11−#13). PQS coordinates of the polynomial coefficients had high standard deviations in the class of whole wheat. This is the reason why parameters #8 (PQS_x) and #9 (PQS_y) were accepted in most cases (Table 40).

Table 40: Rejection of PQS coordinates of polynomial coefficients

Classes:	Foreign	Corn	Small wheat	Whole wheat	Pieces
PQS_x	1.11 %	0.33 %	2.04 %	6.25 %	964
PQS_y	1.48 %	0.33 %	1.02 %	7.29 %	964
Pieces	270	306	196	192	

Corn kernels and foreign materials differ from whole wheat kernels in almost all parameters. Analysis of distances by parameters created a new option: the number of rejected attributes (N_{lim}). In order to select the best value, frequency histograms were computed (Fig.41).

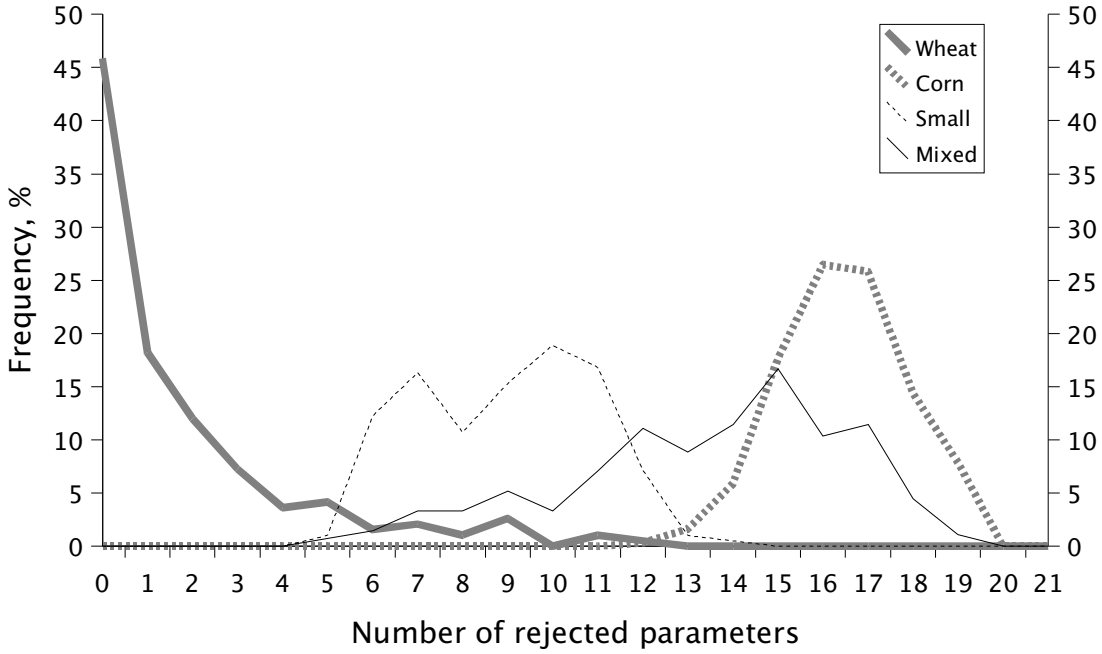

Fig.41: Distribution of samples according to the number of rejected attributes

The advantages of classification of individual parameters with a normalized distance function are:

- easy computation (analysis is based on average values and standard deviations)
- flexible: there are two options for users:
  − limiting value for distance function (D_{lim})
  − limiting value for number of rejected parameters (N_{lim})
- unknown objects are not classified into groups
- there are no restrictions for the knowledge base (number of teaching samples or number of parameters)

However, the effectiveness of this classification method depends on the quality of teaching samples.

6. Summary and conclusions

Visual qualification of objects is generally used in sensory analysis or in sensory analysis based quality control. This type of inspection allocates valuable human resources (requires well−trained people with experience). On the other hand, it is still subjective and repeatability depends on the physical condition of the experts.

Digital image analysis is an objective and nondestructive method for measurement of features such as shape, size and surface texture. Image and data processing algorithms were developed and deployed to fit mathematical functions to shape; reveal regularity, symmetry and complexity of shapes; and to utilize periodic color patterns and color distributions of the surfaces of selected objects. An optimal set of 21 visual parameters was selected:

- 4 parameters for shape estimation with polynomial functions
- 6 parameters to describe symmetry and regularity of shape (3 for attractors and 3 for chaotic maps)
- 3 parameters for color measurement
- 8 parameters to identify patterns of surface texture (2 parameters each for 3 color signals and gray level)

New approaches were presented for

- evaluation of attractors (or delay functions) to measure self−similarity
- symmetry measurement based on difference maps
- evaluation of polynomial function coefficients
- evaluation of difference histograms of surfaces

These parameters were able to distinguish test classes of whole and small wheat, corn kernels, and mixtures of different types of foreign materials with high accuracy. Decision trees − made of pairwise discriminant functions − were built.

A distance function based on average values and standard deviations was introduced and applied successfully. There are two options in this classification procedure:

- a limiting value for distance function
- a limiting value for the number of rejected parameters

Selection of the optimal parameters can vary according to the main goal of classification. Experts can balance risk of rejection and risk of acceptance.

Accurate and objective determination of visual parameters for seed grains and materials other than the primary grain gives additional information and opportunity for research. Computer analysis of image information is useful in development of sorting and cleaning machines, and in optimization of industrial procedures.

6.1 Methodology

The following methods were developed for the special purposes of digital image processing of seed grains and other materials in the sample.

6.1.1 Shape evaluation with sine function of variable period

The following sine function was used to fit polar outline of objects:

$$Y = a + b \cdot \sin(c \cdot x + d)$$

where coefficient *a* means the average radius, *b* means the amplitude, *c* is the period (type of shape) and *d* is the rotation of object in front of the camera.

6.1.2 Shape evaluation with sine function of variable amplitude

The following function was used to model shape of whole wheat grains and distinguish wheat and non−wheat objects.

$$Y = a + (b + c \cdot \sin(x + d))\sin(2x + e)$$

where *a* means the average radius, *b* means the similarity to the elliptic shape, *c* is the size of asymmetry and *d*−*e* computes the position of asymmetric deformation compared to the direction of the major axis.

6.1.2 Polynomial regression

Polynomial of power 8 was used to fit polar outline of objects. As a result of regression, four parameters were calculated: average radius of object, determination coefficient (R^2) and coordinates of quality point of polynomial coefficients.

6.1.3 Self−similarity of shape

Self−similarity of shapes were measured with attractors. These delay functions were generated from the polar outline with 25% shift. Trajectories in the phase space were evaluated with the area of the smallest covering square, area of curve within this square and perimeter index. This novel parameter − perimeter index − is a dimensionless quantity and some sort of density function. It includes the length of perimeter of object with unit radius in the unit area of attractor:

$$PI = \frac{N}{\bar{R} \cdot (r_{max} - r_{min})^2}$$

where *N* means the length of perimeter in pixels, $\bar{R}$ is the average radius and *r* means normalized radius.

6.1.4 Symmetry of shape

Symmetry of shape was measured with difference matrix of polar outline data and its visualization called chaotic map. The following equation transforms polar outline into matrix of differences:

$$M[x;y]=\frac{|R_x-R_y|}{R_{max}-R_{min}}$$

where $M[x;y]$ is the element of matrix, R_x means the radius at angle x, R_{max} is the maximum and R_{min} is the minimum radius. Statistical parameters were used to identify pattern of chaotic maps: uniformity of energy, entropy and homogeneity.

6.1.5 Surface texture

Differences of intensities on the surface of selected object were collected in histograms and Polar Qualification System (PQS) was used to classify them.

6.1.6 Optimal parameter set

Optimal parameter set of 21 attributes was selected to describe objects. This set is consisting of information about shape (10 parameters: result of polynomial regression and chaotic properties), color (3 parameters) and surface pattern (8 parameters: coordinates of polar quality points).

6.1.7 Classification

New classification method was introduced. A distance function − a dimensionless quantity − was used to compare measure values to the average of the teaching sample. The function is as follows:

$$D=\frac{x-\bar{x}}{sd}$$

where D is the distance, x is the value of parameter, $\bar{x}$ means the average value and sd means the standard deviation of parameter in the teaching sample. Classification process used two limiting values: maximum acceptable distance and maximum number of parameters, where value exceeded limit of distance.

6.2 Results and conclusions

6.2.1 Evaluation of methods

The following table presents the effectiveness of discriminant analysis of samples.

Correct recognition of samples

Method	Wheat	Broken wheat	Corn
Color information	80.21%	61.28%	96.75%
Sine function of variable period	90.05%	100%	99.03%
Sine function of variable amplitude	97.51%	96.43%	97.42%
Polynomial regression	96.52%	91.07%	97.42%
Chaotic parameters	99.5%	98.21%	99.68%
Surface pattern (gray scaled)	97.4%	98.18%	94.77%
Surface pattern (all color signals)	100%	100%	100%
Optimal parameter set	100%	98.18%	100%

6.2.2 Evaluation with distance function

The following table presents effectiveness of classification on the basis of normalized distance function.

Correct recognition (D_{max}=3, N_{max}=3)

Wheat	Broken wheat	Corn
100%	89.81%	100%

6.2.3 Relationship between polynomial coefficients

There is quadratic relationship between area of smallest covering rectangle of polar polynomial coefficients and PQS_y coordinate of quality point. The fitted function was:

$$Y = a(x-u)^2 + v$$

6.2.4 Normalization of histogram of surface differences

Normalization of histograms before polar qualification decreases distance between classes. They are too close in this case to distinguish and separate successfully.

7. Acknowledgments

Here, on this page of the thesis I would like to deliver my special thanks to

Professor András Fekete,
my supervisor,

Ferene Firtha,
my colleague, with who I could discuss algorithms
and who motivated me to develop in C/C++ instead of Pascal

David Funk,
visiting professor, who helped to improve my English

all of my colleagues at Department of Physics & Control,
who helped my work and created a familiar atmosphere so that
I could really enjoy my working days from their very beginning to the late ends

my Family for their support

and

the Hungarian National Research Fund,
who sponsored part of my work (OTKA F025730)

8. Publication activity

Textbook:

László Baranyai (2001): Mérnöki számítások C/C++ nyelven (Numeric methods for engineers in C/C++). LSI Oktatóközpont, Budapest (ISBN 963 577 307 2)

Articles in English:

László Baranyai, István Farkas (1998): Shape recognition of different wheat varieties. Proc. of IFAC, Control Applications in Post−Harvest and Processing Technology, Pergamon Elseviere Science, Oxford, 95−97

László Baranyai (1999): Estimating shape of seed grains. Publications of University of Horticulture and Food Industry, vol.58, 49−56

László Baranyai (2001): Classification of seed grains on the basis of their surface pattern. Acta Alimentaria (accepted article)

László Baranyai (2001): Comparison of chaotic properties of shape of seed grains. Hungarian Agricultural Engineering (in press)

László Baranyai (2001): Pattern of chaotic maps. Pattern recognition Letters, Elsevier Science (PATREC 2034)

Full text articles of presentations:

László Baranyai, Ferenc Firtha (1997): Selection of broken kernels by image analysis. Quality Assessment of Plant Products, No.3, 1−4

László Baranyai, Ferenc Firtha (1997): Gabonaszemek szín− és alakjellemzõinek összehasonlítása számítógépes látórendszer felhasználásával. (Comparison of color and shape attributes of seed grains with digital image processing). MTA−AMB Kutatási és Fejlesztési Tanácskozás, Gödöllõ, 274−278

László Baranyai (1998): Búzaszemek alakleíró függvényeinek elemzése (Analysis of mathematical functions to describe shape of wheat grains). MTA−AMB Kutatási és Fejlesztési Tanácskozás, Gödöllõ, 294−297

László Baranyai (2000): Gabonahalmaz összetevõinek vizsgálata felületi mintázatuk alapján (Analysis of surface texture in samples of seed grains). MTA−AMB Kutatási és Fejlesztési Tanácskozás, Gödöllõ

László Baranyai (2000): Visual evaluation of grains. AgEng 2000 Conference Proceedings, Warwick, CD−ROM

László Baranyai (2001): Periodikus jelek kaotikus paramétereinek összehasonlítása (Comparison of chaotic properties of periodic signals). MTA−AMB Kutatási és Fejlesztési Tanácskozás, Gödöllõ

Other articles:

László Baranyai (1999): Kódvita (Discusion on encoding). Új Alaplap, vol.7, 28

László Baranyai (2000): A "házi" kriptográfia (The "home−made" cryptography). Új Alaplap, vol.3, 58−59

Presentations:

László Baranyai (1997): Gabonaszemek szín− és alakjellemzõinek összehasonlítása számítógépes képelemzéssel (Comparison of color and shape attributes of seed grains with digital image processing). OTDK, Keszthely (1st price in section of Food Science)

László Baranyai (1998): Számítógépes alakfelismerési módszerek alkalmazása a minõségbiztositásban (Application of computerized shape recognition in quality control). EOQ Magyar Nemzeti Bizottsága, statisztikai módszerek albizottság ülése, Budapest

Perédi, J. − Szollár, L. − Rischák, K. − Baranyai, L. (1998): A zsírsavöszetétel−módosítás hatása a napraforgóolaj triglicerid−összetételére (Effect of changes in fatty acid content on the triglyceride content of sunflower oil). Lippay János − Vas Károly Tudományos Ülésszak, Budapest

László Baranyai (2000): Termények alakjellemzése kaotikus paramétereikkel (Shape description of grains and vegetables with chaotic parameters). Lippay János − Vas Károly Tudományos Ülésszak, Budapest

László Baranyai (2001): Malomipari alapanyagok minõségének vizsgálata számítógépes látórendszerrel (Digital image processing for quality control in milling industry). EOQ Magyar Nemzeti Bizottsága, statisztikai módszerek albizottság ülése, Budapest

Electronic publications:

László Baranyai (2000): A képfeldolgozás alaplépéseit bemutató program (Basic steps of digital image processing). Új Alaplap, vol.3, CD−ROM

László Baranyai (Internet site): Test images for pattern recognition
http://physics2.kee.hu/baranyai/image.htm (Department of Physics & Control)
(Links can be found at AgEng SIG9 and NJSZT−KÉPAF)

Other:

Baranyai, L − Meuleman, J. (1998): Uborka térbeli helyzetének meghatározása üvegházban (Measurement of three−dimensional position of cucumbers in greenhouse). Lippay János − Vas Károly Tudományos Ülésszak, Budapest (poster)

László Baranyai (1998): Three−dimensional imaging of cucmbers in the greenhouse. TEMPUS Report at IMAG−DLO, Wageningen, NL

László Baranyai (1999): Szemes termények felismerése alak− és felületi jellemzõik alapján (Identification of seed grains on the basis of shape and texture parameters). MTA−AMB Kutatási és Fejlesztési Tanácskozás, Gödöllõ

9. References

F.J. Adamsen, P.J. Pinter Jr., E.M. Barnes, R.L. LaMorte, G.W. Wall, S.W. Leavitt, B.A. Kimball /1999/
Measuring wheat senescence with a digital camera
Crop Science, vol.39, 719−724

H. Bunke, M. Zumbühl /1999/
Acquisition of 2D shape models from scenes with overlapping objects using string matching
Pattern Analysis & Applications, vol.2, 2−9

M.J. Bünner, M. Ciofni, A. Giaquinta, R. Hegger, H. Kantz, R. Meucci, A. Politi /2000/
Reconstruction of systems with delayed feedback: I. Theory
The European Physical Journal, vol.10, 165−176

K.G. Campbell, C.J. Bergman, D.G. Gualberto, J.A. Anderson, M.J. Giroux, G. Hareland, R.G. Fulcher, M.E. Sorrells, P.L. Finney /1999/
Quantitative trait loci associated with kernel traits in a soft x hard wheat cross
Crop Science vol.39, 1184−1195

CIE Central Bureau in Vienna
CIE 15.2−1986 Tables (x,y,z for 2° and 10°; Colour stimulus functions)
http://www.ping.at/CIE

S. Chaturvedi, P.D. Drummond /1999/
Stochastic diagrams for critical point spectra
The European Physical Journal, vol.8, 251−267

Codex Alimentarius Hungaricus 2−61/1997
Milling products

T.G. Crowe, M.J. Delwiche /1996/
A system for fruit defect detection in real−time
AgEng ’96, Madrid, Paper No. 96F−023

EEC No. 2731/75, 29 October 1975
Regulation of standard qualities for common wheat, rye, barley, maize and durum wheat in the European Community

EEC No. 1454/82, 18 May 1982
Regulation of standard qualities for common wheat, rye, barley, maize and durum wheat in the European Community

EEC No. 1028/84, 31 March 1984
Regulation of standard qualities for common wheat, rye, barley, maize and durum wheat in the European Community

EEC No. 2094/87, 13 July 1987
Regulation of standard qualities for common wheat, rye, barley, maize, sorghum and durum wheat in the European Community

EEC No. 689/92, 16 March 1992
Fixing the procedure and conditions for the taking−over of cereals by intervention agencies

EEC No. 2054/93, 19 July 1993
Regulation of standard qualities for common wheat, rye, barley, maize, sorghum and durum wheat in the European Community

EEC No. 2594/97, 18 December 1997
Regulation of standard qualities for common wheat, rye, barley, maize, sorghum and durum wheat in the European Community

R.P. Ewing, R. Horton /1999/
Quantitative color image analysis of agronomic images.
Agronomy Journal, vol.91, 148−153

Federal Grain Inspection Service /1999/
1998 U.S. grain exports: quality report
U.S. Department of Agriculture, 1−4; 21−22; 35−37

F. Firtha /1998/
Természetes objektumok alakjának leírása (Description of shape of natural objects)
János Lippay − Károly Vas International Scientific Symposium, Budapest

J. Gleick /2000/
Káosz. Egy új tudomány születése (Chaos. Making a new science)
Göncöl Kiadó, Budapest

Z. Gyõri, I. Mile Gyõriné /1998/
A búza minõsége és minõsítése (Quality and qualification of wheat)
Mezõgazdasági Szaktudás Kiadó, Budapest

Y.J. Han, Y. Feng, C.L. Weller /1996/
Frequency domain image analysis for detecting stress cracks in corn kernels
Applied Engineering in Agriculture, vol.12, 487−492

R.M. Haralick, L.G. Shapiro /1992/
Computer and robot vision.
Addison−Wesley Publishing Company, Inc., 453−505

B. Jähne, H. Haußecker, P. Geißler /1999a/
Handbook of computer vision and applications. Volume 1. Sensors and Imaging.
Academic Press, San Diego

B. Jähne, H. Haußecker, P. Geißler /1999b/
Handbook of computer vision and applications. Volume 2. Signal processing and pattern recognition.
Academic Press, San Diego

B. Jähne, H. Haußecker, P. Geißler /1999c/
Handbook of computer vision and applications. Volume 3. Systems and applications.
Academic Press, San Diego

K.J. Kaffka, L.S. Gyarmati /1998/
Investigating the polar qualification system
Journal of Near Infrared Spectroscopy, vol.6, A191−A200

K. Liao, M.R. Paulsen, J.F. Reid, B.C. Ni, E.P. Bonifacio−Maghirang /1993/
Corn kernel breakage classification by machine vision using a neural network classifier
Transactions of the ASAE, vol.36, 1949−1953

Gy. Lukács /1982/
Színmérés (Colorimetry)
Mûszaki Könyvkiadó, Budapest, 131−134; 142

S. Majumdar, D.S. Jayas /2000/
Classification of cereal grains using machine vision: I. Morphology models
Transactions of the ASAE, vol.43, 1669−1675

S. Majumdar, D.S. Jayas /2000/
Classification of cereal grains using machine vision: II. Color models
Transactions of the ASAE, vol.43, 1677−1680

S. Majumdar, D.S. Jayas /2000/
Classification of cereal grains using machine vision: III. Texture models
Transactions of the ASAE, vol.43, 1681−1687

S. Majumdar, D.S. Jayas /2000/
Classification of cereal grains using machine vision: IV. Combined morphology, color and texture models.
Transactions of the ASAE, vol.43, 1689−1694

D.R. Marshall, F.W. Ellison, D.J. Mares /1984/
Effects of grain shape and size on milling yields in wheat. I. Theoretical analysis based on simple geometric models.
Australian Journal of Agricultural Research vol.35, 619−630
D.R. Marshall, D.J. Mares, H.J. Moss, F.W. Ellison /1986/
Effects of grain shape and size on milling yields in wheat. II. Experimental studies
Australian Journal of Agricultural Research vol.37, 331−342
L. Martinovich, J. Felföldi /1996/
Measurement of homogeneity of onion (*Allium cepa L.*) varieties and lines using computer based shape and colour analyses.
Horticultural Science, vol.28., 69−75
MathWorks Inc. /2000/
Image processing toolbox. User's guide
The MathWorks, Inc.
J. Meuleman, C. van Kaam /1997/
Unsupervised image segmentation with neural networks
3rd International Conference on Sensors in Horticulture, Tiberias, Israel
T. Morimoto, T. Takeuchi, H. Miyata, Y. Hashimoto /1998/
Pattern recognition of fruit shape on the basis of chaos using neural networks
CAPPT 2nd International Workshop, Budapest, 125−130
MSZ 6354/1−1989
MSZ 6354/2−82
MSZ 6367:2001
MSZ 6383
H. Naumann, G. Schröder /1983/
Bauelemente der Optik. Taschenbuch für Konstrukteure
Carl Hanser Verlag München Wien, 391
M.R. Neuman, H.D. Sapirstein, E. Shwedyk, W. Bushuk /1989/
Wheat grain colour analysis by digital image processing I. Methodology
Journal of Cereal Science, vol.10, 175−182
M.R. Neuman, H.D. Sapirstein, E. Shwedyk, W. Bushuk /1989/
Wheat grain colour analysis by digital image processing II. Wheat class discrimination
Journal of Cereal Science, vol.10, 183−188
G. Palubinskas, R.M. Lucas, G.M. Foody, P.J. Curran /1995/
An evaluation of fuzzy and texture−based classification approaches for mapping regenerating tropical forest classes from Landsat−TM data
International Journal of Remote Sensing, vol.16, 747−759
J.R. Piggott /1986/
Statistical procedures in food research
Elsevier Applied Science Publishers Ltd., Essex
Gy. Popper, F. Csizmás /1993/
Numerikus módszerek mérnököknek (Numeric methods for engineers)
Akadémiai Kiadó
A. Rosenfeld /2000/
Image analysis and computer vision. The past half−century
IAPR Newsletter vol.22, No.1,
J. Schanda /2000/
Colorimetry (in: Handbook of Applied Colorimetry, edited by C. DeCusatis)
Am. Inst. of Physics, Woodbury, New York, 327−412
H. Schneider, M. Häußer, H.D. Kutzbach /1997/
Optimize grain quality by broken kernel detection
Quality Assessment of Plant Products, 25−28

P. Shatadal, D.S. Jayas, J.L. Hehn, N.R. Bulley /1995/
Seed classification using machine vision
Canadian Agricultural Engineering vol.37, No.3, 163−167
P. Shatadal, D.S. Jayas, N.R. Bulley /1995/
Digital image analysis for software separation and classification of touching grains: I. Disconnect algorithm
Transactions of the ASAE, vol.38, 635−643
P. Shatadal, D.S. Jayas, N.R. Bulley /1995/
Digital image analysis for software separation and classification of touching grains: II. Classification
Transactions of the ASAE, vol.38, 645−649
R. Singh, V.M. Maru, P.S. Moharir /1998/
Complex chaotic system and emergent phenomena
Journal of Nonlinear Science, vol.8, 235−259
T. Szirányi, J. Zerubia /1997/
Markov random field image segmentation using cellular neural network
IEEE Transactions on Circuits and Systems, vol.44, 86−89
R.K. Tiwari, K.N.N. Rao /1999/
Phase space structure, attractor dimension, Lyapunov exponent and nonlinear prediction from Earth's atmospheric angular momentum time series
Pure and Applied Geophysics, vol.156, 719−736
United States Grain Standard Act
T. Vízhányó /1999/
PQS method for analysis of mushroom spectral characteristics
Publ. Univ. Horticulture and Food Industry, vol.58, 27−34
I.Y. Zayas, C.R. Martin, J.L. Steele, A. Katsevich /1996/
Wheat classification using image analysis and crush−force parameters
Transactions of the ASAE, vol.39, 2199−2204
I. Zayas, Y. Pomeranz, F.S. Lai /1989/
Discrimination of wheat and nonwheat components in grain samples by image analysis
Journal of Cereal Chemistry, vol.66, 233−237

10. Magyar nyelvû összefoglaló és tézisek

A látható tulajdonságok alapján történõ minõsítés általánosan használt az érzékszervi bírálatokban, vagy az arra épülõ minõsítõ rendszerekben. Ez a fajta vizsgálat jelentõs erõforrást igényel (jól képzett szakembereket igényel). Másrészt szubjektív és ismételhetõsége a minõsítést végzõ személy fizikai állapotától függ.

A digitális képfeldolgozás objektív és roncsolásmentes módszert nyújt olyan tulajdonságok mérésére, mint a forma, méret és a felszín mintázata. Képfeldolgozó és egyéb matematikai algoritmusok kidolgozására került sor, amelyek függvényeket illesztenek, mérik az alak önhasonulását és szimmetriáját, valamint leírják a kiválasztott test felszínén látható periodikus mintákat. A következõ − 21 paraméterbõl álló − halmaz írta le legjobban az objektumokat:

- 4 paraméter az alak leírására polinomiális regresszióval
- 6 paraméter a szimmetria és önhasonlóság mérésére (3 az attraktorok és 3 a káosztérképek értékeléséhez)
- 3 paraméter a szín meghatározáshoz
- 8 paraméter a felszín mintázatának azonosításához (2 paraméter minden színjellemzõhöz és a szürke képhez)

Új módszereket sikerült kifejleszteni

- az attraktorok kiértékelésére és az önhasonulás mérésére
- a szimmetria mérésére a különbségmátrix alapján
- a polinomiális regresszió együtthatóinak értékelésére
- a felszín különbség−hisztogramjainak értékelésére

Ezekkel a paraméterekkel sikeresen megkülönböztethetõek a búza−, kukoricaszemek és a mintákban található idegen anyagok. A páronként elvégzett diszkriminancia analízis segítségével döntési fát lehetett felépíteni.

Egy − az átlag és szórás értékeken alapuló − távolságfüggvény is hatékonynak bizonyult. Az osztályozás két változóval szabályozható:

- a távolság függvény megengedett legnagyobb értéke
- a megengedett határértéknél távolabbi paraméterek száma

Az optimális értékek igen különbözõek lehetnek az osztályozás céljától függõen. A szakértõk maguk dönthetnek az elfogadás és elutasítás kockázatainak súlyáról.

A gabonaszemek és egyéb − a mintákban megtalálható − anyagok vizuális tulajdonságainak pontos és objektív leírása többletinformációval láthatja el a kutatásokat. Ezen felül a vizuális információk elemzése hasznos lehet a válogató− és tisztító berendezések fejlesztésekor, valamint az ipari folyamatok optimálása során.

10.1 Módszerek fejlesztése

A következõ módszerek fejlesztése segítette a gabonaszemek és a mintákban levõ egyéb anyagok digitális képfeldolgozással történõ elemzését.

10.1.1 Alak vizsgálata változó periódusú szinusz függvénnyel

A következõ matematikai függvény jól illeszkedett a polárkoordinátás adatokra:

$$Y = a + b \cdot \sin(c \cdot x + d)$$

ahol *a* jelenti az átlagos sugarat, *b* jelenti az amplitúdót, *c* a periódust (egyben a jellemzõ formát), valamint *d* azonosítja a tárgy kamera elõtti pozícióját.

10.1.2 Alak vizsgálata változó amplitúdóval rendelkezõ szinusz függvénnyel

A következõ matematikai függvény egy deformált elliptikus alakot illeszt a körvonalra. Ez a forma a búzaszemekre jellemzõ.

$$Y = a + (b + c \cdot \sin(x + d)) \sin(2x + e)$$

ahol *a* jelenti az átlagos sugarat, *b* az ellipszishez való hasonlóságot, *c* a forma szimmetriájának mértékét, valamint $d - e$ megmutatja az aszimmetrikus deformáció pozícióját a test fõtengelyéhez viszonyítva.

10.1.3 Polinomiális regresszió

Nyolcadfokú polinom illesztésének erdményeként a következõ paraméterek írják le a formát: átlag sugár, determinációs együttható (R^2) és az illesztett polinom együtthatóinak polár minõségpontjának koordinátái.

10.1.4 Az alak önhasonulása

Az alak önhasonulása attraktorok segítségével vált mérhetõvé. A késleltetési függvények a polár adatsor 25%−os eltolásával jöttek létre. A fázistérben megjelenõ gráfot a következõ paraméterek írják le: a gráfot befoglaló legkisebb négyzet területe, a gráf által lefedett terület aránya a négyzeten belül, valamint a kerületi index. Ez utóbbi egy új paraméter, egy sûrûség jellegû dimenziómentes mérõszám. Megmutatja, hogy az egységnyi méretû test gráfjának mekkora része esik az attraktort befoglaló terület egységnyi részletére.

$$PI = \frac{N}{\bar{R} \cdot (r_{max} - r_{min})^2}$$

ahol *N* jelenti a kerület hosszát képpontokban, $\bar{R}$ az átlag sugarat, és *r* a normált sugár értékeket.

10.1.5 A forma szimmetriája

Az alak szimmetriája a polár adatsorból elõállított különbségmátrix, valamint annak megjelenített képébõl (káosztérkép) a mintázat elemzésével megállapítható. A következõ egyenlet bemutatja a mátrix elemeinek kiszámításához használt összefüggést:

$$M[x;y]=\frac{|R_x-R_y|}{R_{max}-R_{min}}$$

ahol $M[x;y]$ a mátrix egy eleme, R_x jelenti az x szöghöz tartozó sugár értékét, R_{max} a legnagyobb és R_{min} a legkisebb sugár. A mátrix mintázatának kiértékelése az energia egyenletessége, entrópia és homogenitás statisztikai jellemzõkkel végezhetõ el.

10.1.6 Felszíni mintázat elemzése

A felszín szomszédos pontjainak intenzitás különbségeit hisztogramba gyûjtve a polár minõsítõ renszer (PQS) hatékonynak bizonyult a mintázatok azonosításában.

10.1.7 Optimális paraméterek

Összesen 21 elembõl álló paraméter csoport kiválasztásával sikerült leírni a testek vizuális jellemzõit. A csoport tartalmazza az alaki jellemzõket (10 paraméter: a polinomiális regresszió eredményeként és a káosz leírásával), színjellemzõket (3 paraméter), valamint a felszín leírását (8 paraméter: a minõségpont két koordinátája minden színjellemzõre és az intenzitás értékekre).

10.1.8 Osztályozás

Új osztályozó eljárást sikerült bevezetni. Egy dimenziómentes mérõszám segítségével a mért paraméterek a tanuló minták középértékeihez hasonlíthatóak:

$$D=\frac{x-\bar{x}}{sd}$$

ahol D a távolság, x a paraméter mért értéke, $\bar{x}$ a tanulóminta középértéke és sd a paraméter értékeinek szórása. Az osztályozó algoritmus viselkedése két adattal szabályozható: a távolságok elfogadható legnagyobb értéke és ezt a határértéket meghaladó paraméter értékek számának maximuma.

10.2 Eredmények és következtetések

10.2.1 Módszerek értékelése

A következõ táblázat foglalja össze az alkalmazott módszerek hatékonyságát diszkriminancia analízissel történõ osztályozás során.

A minták felismerésének hatékonysága

Módszer	Búza	Törött szem	Kukorica
Szín jellemzõk	80.21%	61.28%	96.75%
Változó periódusú szinusz függvény	90.05%	100%	99.03%
Változó amplitúdójú szinusz függvény	97.51%	96.43%	97.42%
Polinomiális regresszió	96.52%	91.07%	97.42%
Kaotikus jellemzõk	99.5%	98.21%	99.68%
Felszíni mintázat (szürke)	97.4%	98.18%	94.77%
Felszíni mintázat (összes színre)	100%	100%	100%
Optimális paraméterek	100%	98.18%	100%

10.2.2 Evaluation with distance function

A következõ táblázat bemutatja az osztályozás hatékonyságát a normált távolságfüggvény felhasználásával.

Felismerés hatékonysága (D_{max}=3, N_{max}=3)

Búza	Törött szem	Kukorica
100%	89.81%	100%

10.2.3 Polinomiális együtthatók kapcsolata

Négyzetes összefüggés van a polinom együtthatóinak polár diagramját befoglaló téglalap területe és a gráf minõségpontjának PQS_y koordinátája között. Az illesztett függvény egyenlete:

$$Y = a(x-u)^2 + v$$

10.2.4 A felszíni különbségek hisztogramjának normálása

A polár minõsítõ rendszer alkalmazása elõtt elvégzett normálás hatására a csoportok minõségpontjai túlságosan közel kerülnek egymáshoz. Ez a közelség csökkenti a csoportok felismerésének és megkülönböztetésének hatékonyságát.